Title
The Mitochondrial Iron-Sulfur Cluster Protein BOLA3 in Beta Cell Metabolism and Function

Author
Kerper, Natanya R

Publication Date
2021

Peer reviewed|Thesis/dissertation

The Mitochondrial Iron-Sulfur Cluster Protein BOLA3 in Beta Cell Metabolism and Function

by

Natanya Kerper

DISSERTATION

Submitted in partial satisfaction of the requirements for degree of

DOCTOR OF PHILOSOPHY

in

Biomedical Sciences

in the

GRADUATE DIVISION

of the

UNIVERSITY OF CALIFORNIA, SAN FRANCISCO

Approved:

DocuSigned by:
Ethan Weiss
7508BE9540AA44B...

Ethan Weiss

Chair

DocuSigned by:
Gregory Ku

Gregory Ku

DocuSigned by:
Matthias Hebrok
4172DABAAE5543A...

Matthias Hebrok

Committee Members

Dedication

This work is dedicated to Terry and Maryellen Tucker.

Acknowledgements

I would like to acknowledge my PhD mentor, Matthias Hebrok, and my thesis committee members, Ethan Weiss and Greg Ku. Without their support this dissertation wouldn't have been possible.

I would like to acknowledge the friends and research colleagues who got me through this whole process. I asked you for advice; I confided in you; I cried on your shoulders and leaned on you when I couldn't stand. There are no words for how grateful I am to all of you.

I would like to acknowledge my family: my brother, Joseph, and my mother, Carla. Joe, you always saw me as more capable than I saw myself—I know you're proud of me, and I hope you know that I'm just as proud of you. Mom, I owe the best of who I am today to you. Your love and support carried me through my toughest moments. I hope you know that, too.

Finally—and more than anything—I would like to acknowledge my fiancée, Sara. You always saw a path forward, even when I couldn't. I love you, I love you, I love you—and I can't wait to spend the rest of our lives telling you that.

Abstract

The Mitochondrial Iron-Sulfur Cluster Protein BOLA3

in Beta Cell Metabolism and Function

Natanya R. Kerper

Beta cell dysfunction is a major contributor to the pathogenesis of type 2 diabetes. This dysfunction, which results in the inability of the beta cell to produce and secrete insulin upon elevations in blood glucose, has been linked to various metabolic and mitochondrial insults. It has been previously been shown that perturbations of the iron metabolism and mitochondrial iron-sulfur (Fe-S) cluster biogenesis and transport may lead to beta cell dysfunction; we therefore sought to explore the role of the mitochondrial Fe-S cluster protein BOLA3 in beta cell metabolism and function. In this study we determine that beta cell-specific loss of *Bola3* in both murine and human beta cells results in a gradual perturbation of glucose homeostasis and beta cell degradation. Our data further indicate that both treatment with exogenous recombinant BOLA3 protein and supraphysiological expression of endogenous *Bola3* improves glucose-stimulated insulin secretion in beta cells, thereby establishing a potential therapeutic role for *Bola3* and other regulators of mitochondrial metabolism in type 2 diabetes.

Table of Contents

Chapter 1. Background and Introduction……..1

Diabetes and the Beta Cell……1

The Beta Cell and Insulin Secretion……..2

Insulin Secretion and Aerobic Respiration……2

Iron and Mitochondria in the Beta Cell……..3

Fe-S Cluster Biogenesis……..4

The Mitochondrial Fe-S Cluster Protein BOLA3……..5

Chapter 2. The role of BOLA3 in the murine beta cell……9

Introduction……9

Results……9

Bola3^{KO} mice exhibit dysfunctional glucose homeostasis in vivo……9

Loss of *Bola3* results in beta cell dedifferentiation……17

Islets deficient in *Bola3* demonstrate mitochondrial fragility and decreased cellular respiration……..21

Discussion……23

Chapter 3. Recombinant murine BOLA3 protein as a novel beta cell secretagogue…..25

Introduction……..25

Results……25

Discussion……28

Chapter 4. The role of BOLA3 in the human beta cell……..30

Introduction……..30

Results……31

Correlation between BOLA3 and cellular maturity in human beta cells….31

CRISPR-Cas9 ablation of *Bola3* in human stem cell-derived beta cells...37

Inducible *Bola3* overexpression in human stem cell-derived beta cells…44

Discussion……52

Chapter 5. Materials and Methods……..54

Works Cited…….62

List of Figures

Figure 1-1. Fe-S cluster biogenesis……...5

Figure 1-2. BOLA3 pathway and targets in the mitochondria……8

Figure 2-1. BOLA3 expression is restricted to the beta cell in the adult murine pancreas……..…10

Figure 2-2. A mouse model of *Bola3* knockout……..12

Figure 2-3. *Bola3*^{KO} mice exhibit dysfunctional glucose homeostasis *in vivo*……...14

Figure 2-4. *Bola3*^{KO} mice display late-stage fasting hyperinsulinemia and increased body weight without concurrent insulin resistance……16

Figure 2-5. Loss of Bola3 results in downregulation of canonical beta cell markers…...18

Figure. 2-6. Altered alpha cell number and distribution in *Bola3*^{KO} islets……..20

Figure 2-7. Mitochondrial fragility and decreased cellular respiration in *Bola3*-deficient islets……..22

Figure 3-1. Recombinant BOLA3 protein augments murine islet insulin secretion in a dose-dependent manner……...27

Figure 3-2. Recombinant BOLA3 protein augments human islet insulin secretion…….28

Figure 4-1. BOLA3 localizes to endocrine cells within the human pancreas……32

Figure 4-2. Enriched beta clusters possess contain more BOLA3 than immature, beta-like clusters…….33

Figure 4-3. Upregulation of iron-sulfur cluster and mitochondrial respiratory chain complex genes correlates with cellular maturity……35

Figure 4-4. Generation of the CRISPR-based inducible *BOLA3* knockout hESC line……...38

Figure 4-5. Doxycycline treatment regimen of BOLA3^{KO} clusters……..39

Figure 4-6. Validation of the *BOLA3*^{KO} line……40

Figure 4-7. BOLA3 knockout in eBCs results in diminished insulin secretion……..42

Figure 4-8. Generation of the BOLA3^{OE} overexpression hESC line……..45

Figure 4-9. Treatment and analysis timeline of Bola3^{OE} eBCs……46

Figure 4-10. Validation of the *BOLA3*^{OE} line……..47

Figure 4-11. Overexpression of BOLA3 in Day 27 BOLA3^{OE} eBCs improves glucose-stimulated insulin secretion……49

Figure 4-12. Overexpression of BOLA3 in Day 34 BOLA3^{OE} eBCs improves glucose-stimulated insulin secretion……51

CHAPTER 1.

Introduction & Background

Diabetes and the Beta Cell

Pancreatic beta cells are vital to the maintenance of systemic glucose homeostasis. In response to elevated blood glucose levels, beta cells secrete the peptide hormone insulin, which stimulates glucose uptake by peripheral tissues such as skeletal muscle, liver, and adipose tissue. Tight regulation of insulin secretion is critical; inappropriately high serum insulin results in low blood glucose, or hypoglycemia, which poses a significant immediate health risk. In contrast, perturbation of beta cell function and insulin secretion results in diabetes and its associated long-term complications.

The most prevalent and well-characterized forms of diabetes are type 1 diabetes and type 2 diabetes, which account for nearly all diagnosed cases; however, there exist multiple additional subtypes, including the mono-genetic mature onset diabetes of the young (MODY) and transient gestational diabetes. Type 1 diabetes is an autoimmune disease caused by the inappropriate destruction of beta cells by activated immune cells. This wholesale elimination of beta cells results in a near-complete lack of circulating insulin, necessitating treatment with exogenous insulin or a whole-pancreas or islet transplant. Type 2 diabetes, which affects approximately 10.5% of the United States population (National Diabetes Statistics Report), is driven by two primary factors: an acquired resistance to insulin by the peripheral tissues responsible for glucose uptake and beta cell dysfunction (Kahn, 2003; Kahn et al., 2006; Cerf, 2013; Cohrs et al., 2020). Characterized by the inability of the beta cell to secrete appropriate quantities of insulin in response to elevated blood glucose levels, beta cell dysfunction has been

shown to result from a wide variety of physiological stressors, including glucotoxicity (Dingreville et al., 2019; Shyr et al., 2019), cellular hypoxia (Cantley et al., 2008; Puri et al., 2009; Sato et al., 2014), and oxidative stress (Guo et al., 2013; Besseiche et al., 2018).

The Beta Cell and Insulin Secretion

Glucose-stimulated insulin secretion (GSIS) occurs when beta cells sense and absorb excess glucose from the bloodstream through the GLUT1 or GLUT2 glucose transporters and rapidly internalized to generate ATP. The resulting increase in the intracellular ATP/ADP ratio induces closure of K_{ATP}-sensitive channels and plasma membrane depolarization, causing Ca^{2+} channels along the cell surface to open. The subsequent influx of Ca^{2+} ions induces exocytosis of insulin granules from the beta cell interior (Deeney et al., 2000; Kahn et al., 2006; Fu et al., 2013). Insulin secretion is biphasic: first-phase insulin secretion consists of a rapid spike within the initial minutes of glucose challenge, while second-phase insulin secretion entails diminished, but sustained secretion (Seino et al., 2011).

Insulin Secretion and Aerobic Respiration

Insulin secretion, particularly first-phase insulin secretion, requires the beta cell to rapidly and substantially increases ATP production. This results in an increased susceptibility to mitochondrial dysfunction, as more than 95% of ATP in the beta cell is produced within the mitochondria through aerobic respiration (Tarasov et al., 2004). Aerobic respiration is characterized by glycolysis and two additional stages, both of which occur within the mitochondria. The tricarboxylic acid (TCA) cycle oxidizes acetyl-

CoA in the mitochondrial matrix to generate activated electron carriers, which pass electrons to proteins embedded in the mitochondrial respiratory chain for use in the end-stage process of oxidative phosphorylation (Alberts et al., 2002). Studies have linked various metabolic and mitochondrial insults to beta cell dysfunction (Lu et al., 2010; Supale et al., 2013; Thivolet et al., 2017). However, this phenomenon has largely been studied in the context of mtDNA-linked mitochondrial diabetes, pre-existing type 2 diabetes, or concurrent insulin resistance (Maechler and Wollheim, 2001; Supale et al., 2012; Mulder, 2017; Fex et al., 2018). The potential causative role of beta cell-specific mitochondrial impairment, particularly unrelated to broad mtDNA defects, in the development of type 2 diabetes is less well studied.

Iron and Mitochondria in the Beta Cell

Iron is critical to mitochondrial function and aerobic respiration: four of the five mitochondrial respiratory chain complexes and various components of the TCA cycle either directly or indirectly require iron-sulfur (Fe-S) clusters or heme (Paoletti, 2012). However, excess cellular iron is known to inflict oxidative damage through the production of reactive oxygen species (ROS). Iron uptake, storage, and utilization are therefore tightly-regulated processes, particularly in tissues with high metabolic requirements, including the brain and heart. The beta cell differs from these tissues in that its metabolic burden fluctuates with physiological demand for insulin rather than remaining constant; nevertheless, as previously discussed, the process of insulin secretion necessitates a significant amount of cellular respiration, and therefore iron metabolism. In accordance with the dual nature of iron as both necessary and detrimental in excess, iron overload and deficiency have both been associated with beta

cell dysfunction and diabetes, though most current research has focused on iron overload (Swaminathan et al., 2007; Cnop et al., 2013; Simcox and McClain, 2013; Backe et al., 2016; Clark et al., 2018).

Fe-S Cluster Biogenesis

One of the most predominant uses for cellular iron is the production of iron-sulfur (Fe-S) clusters. Fe-S clusters are widely recognized as one of the oldest and most versatile classes of inorganic cofactors (Lill et al., 2009). Their capacity to participate in redox reactions and electron transfer, confer protein stability, donate sulfur ions, and act as environmental sensors makes them critical to organisms across all domains of life (Lill et al., 2006; Levi et al., 2009; Lane et al., 2015). Fe-S cluster biogenesis requires a complex, coordinated effort by a variety of protein components. These include ISCU, the primary dedicated scaffold protein; NFS1, a cysteine desulfurase, and its stabilizing accessory protein LYRM4; and frataxin, a putative mitochondrial iron transporter (Lane et al., 2015). Following assembly on the ISCU scaffold, Fe-S clusters must be transferred to recipient apoproteins. This can be accomplished via one of two mechanisms: direct transfer of the Fe-S clusters to recipient proteins by the HSC20-HSPA9 co-chaperone complex, which associates with ISCU, or indirect transfer via intermediate transport proteins such as NFU1, BOLA3, and IBA57 (Rouault, 2015) (Fig. 1-1). Much remains to be elucidated about the biology of these intermediate transport proteins, the existence of which has only come to light within the last several years; however, they appear to differ primarily on the basis of their capacity to carry particular Fe-S cluster variants (such as [2Fe-2S] and [4Fe-4S] clusters), their target apoproteins,

and their cell-type specificity (Rouault and Tong, 2008; Cameron et al., 2011; Lebigot et al., 2017).

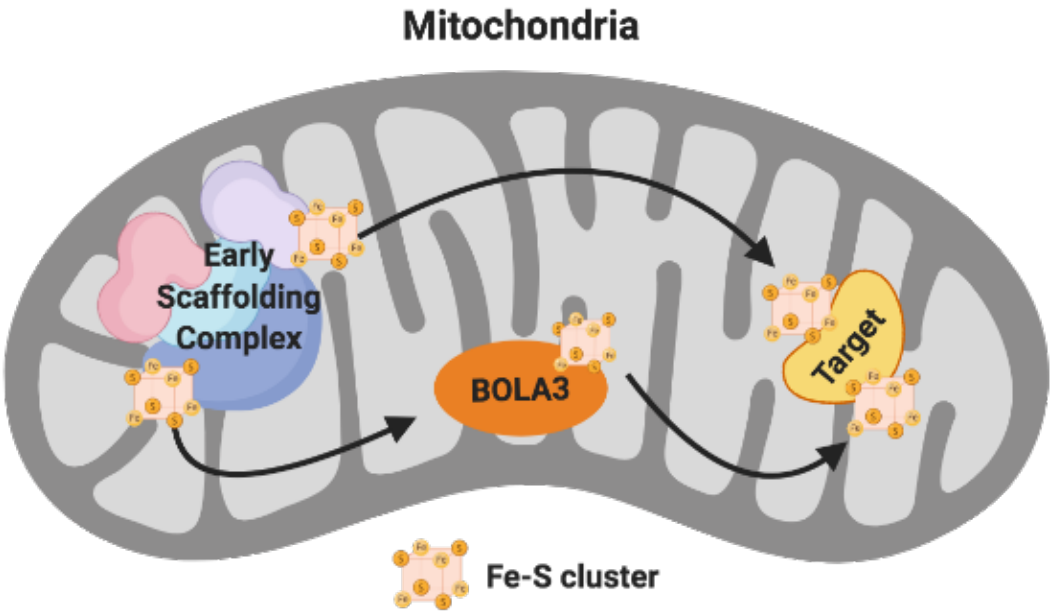

Figure 1-1. Fe-S cluster biogenesis. Fe-S clusters are initially assembled on an early scaffolding complex consisting of ISCU, NFS1, LYRM4, and frataxin. Following assembly on the ISCU scaffold, Fe-S clusters can be transferred to recipient apoproteins via either direct transfer of the Fe-S by the HSC20-HSPA9 co-chaperone complex, which associates with ISCU or indirect transfer via intermediate transport proteins such as BOLA3. Figure created with Biorender.com.

The Mitochondrial Fe-S Cluster Protein BOLA3

Only recently has the role of the Fe-S cluster protein BOLA3 in various aspects of aerobic respiration begun to be elucidated. While little is understood about BOLA3, it is known to serve as an intermediate transport protein in the Fe-S cluster pathway,

responsible for delivering Fe-S clusters to proteins within the mitochondria (Rouault, 2015). In particular, BOLA3 target proteins include those critical to multiple stages of aerobic respiration, including the TCA cycle, which oxidizes acetyl-CoA in the mitochondrial matrix to generate activated electron carriers, and the electron transport chain (ETC), where mitochondrial respiratory chain complexes embedded in the inner mitochondrial membrane accept electrons for use in the end-stage process of oxidative phosphorylation. Lipoic acid synthase (LIAS) utilizes Fe-S clusters delivered by BOLA3 as sulfur donors in the biosynthesis of lipoic acid (Mayr et al, 2014). Multiple steps of the TCA cycle are carried out by enzymatic complexes that require a lipoic acid cofactor for maturation and function, such as the pyruvate dehydrogenase complex (PDH) and alpha-ketoglutarate dehydrogenase complex (aKGDH). Both PDH and αKGDH contain three protein subunits: E1, E2, and E3 (Randle et al., 1983; Yeamen at el., 1989). Following its production, lipoic acid is transferred from LIAS to the E2 subunit of either PDH or aKGDH by the LIPT1 transport protein. BOLA3 has also been implicated in the function of mitochondrial respiratory chain (MRC) protein complexes I, II, and III. Each of these three enzymatic complexes is comprised of between four and forty-four subunits, several of which directly require Fe-S clusters delivered by BOLA3 to perform redox reactions with electrons donated by NADH (Fig. 1-2).

In accordance with its role in mitochondrial respiration, *BOLA3* is expressed across a variety of tissue types (Fagerberg et al., 2014; Uhlén et al., 2015), though levels vary greatly. Importantly, while there are two other BOLA family members, BOLA1 and BOLA2, they are functionally and spatially distinct from BOLA3 (Willems et al., 2013; Banci et al., 2015; Giannuzzi et al., 2019). Further evidence for the inability of other BOLA or Fe-S cluster transport proteins, such as NFU1, to compensate for

BOLA3 loss comes from studies in which homozygous recessive loss-of-function mutations in the BOLA3 gene result in a severe and ultimately fatal condition known as multiple mitochondrial dysfunctions syndrome (MMDS). BOLA3 deficiency results in early lethality and most significantly impacts tissues with high metabolic demand, including the brain and heart: individuals with MMDS present with a wide range of complications including encephalopathies, cardiomyopathies, and lactic acidosis (Cameron et al., 2011; Haack et al., 2013; Ahting et al., 2015). Interestingly, studies have indicated that these patients exhibit hyperglycemia, suggesting a potential link between BOLA3 and beta cell function.

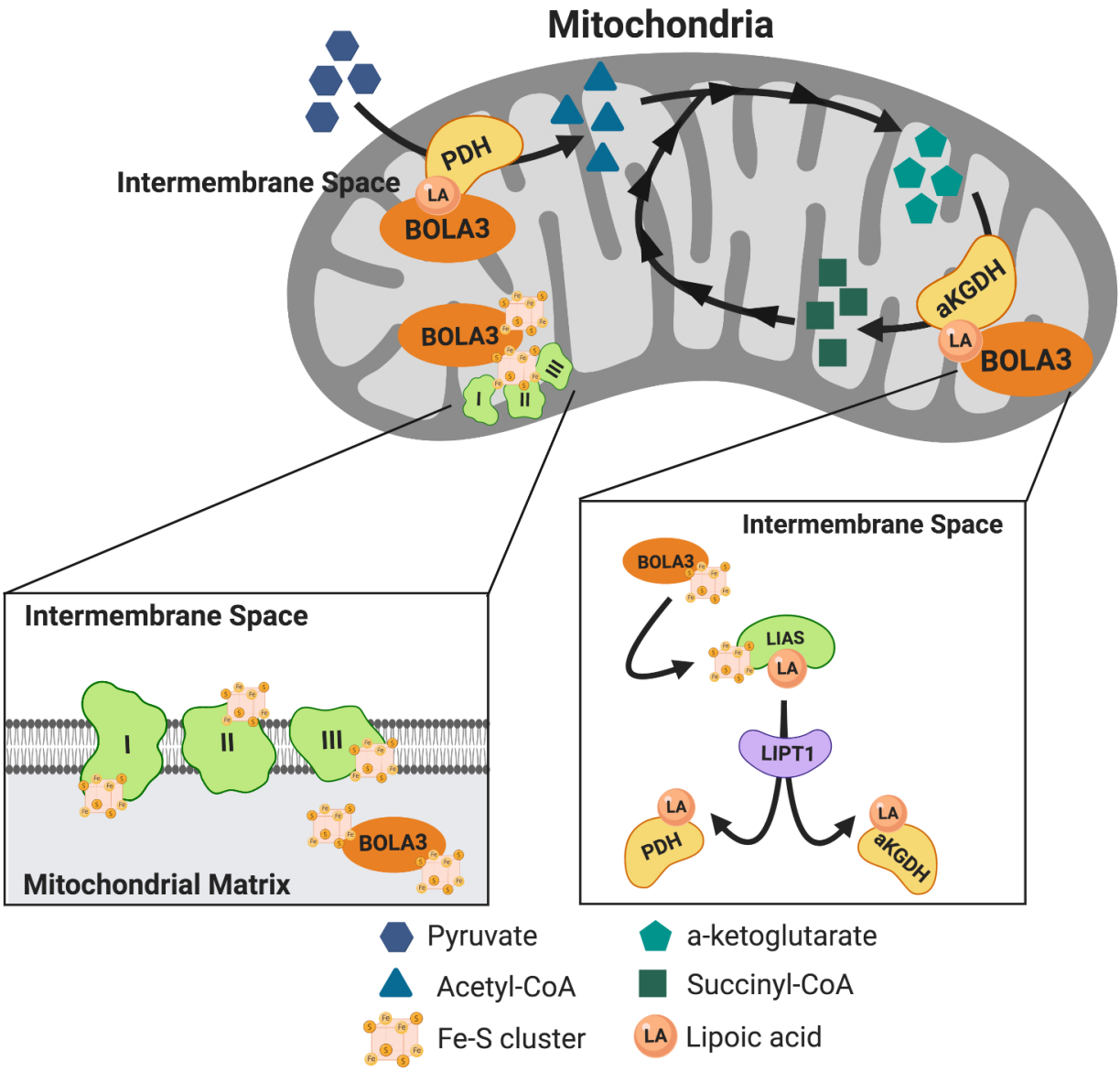

Figure 1-2. BOLA3 pathway and targets in the mitochondria. BOLA3 delivers Fe-S clusters to mitochondrial respiratory chain complexes I, II, and III (right), and lipoic acid synthase (LIAS, left). LIAS utilizes Fe-S clusters in the biosynthesis of lipoic acid, which is then transported by LIPT1 to the pyruvate dehydrogenase (PDH) and alpha-ketoglutarate dehydrogenase (αKGDH) enzymatic complexes, which process various metabolites critical to the TCA cycle. Figure created with Biorender.com.

CHAPTER 2.

The role of BOLA3 in the murine beta cell

Introduction:

The Fe-S cluster protein BOLA3 has emerged as a mediator of multiple aspects of aerobic respiration, including the TCA cycle and oxidative phosphorylation. While clinical research of *Bola3*-deficient MMDS patients is largely restricted to brain and cardiac defects, hyperglycemia has been previously observed. However, MMDS represents a whole-body loss of *Bola3*; it therefore remains unclear the degree to which this effect is a function of peripheral tissue defects, beta cell dysfunction, or both. This lack of specificity, combined with the early lethality of MMDS and scarcity of MMDS patient samples, led us to utilize the mouse as a model system for *in vivo* interrogation of the physiological role and importance of *Bola3* in the beta cell.

Results:

Bola3$^{\beta KO}$ mice exhibit dysfunctional glucose homeostasis in vivo

We first sought to assess the presence of BOLA3 in the murine pancreas. Immunofluorescent staining of wild-type, adult pancreata indicated that BOLA3 is highly detectable in the islet, but not in the acinar or ductal cells that comprise the exocrine compartment. Furthermore, BOLA3 protein localized to insulin+ beta cells, but not glucagon+ alpha cells or somatostatin+ delta cells, suggesting a uniquely high requirement for BOLA3 within the beta cell versus other endocrine cell types (Fig. 2-1). These data would appear to be in accordance with prior research suggesting that beta

cells both express more *Bola3* and engage more extensively in iron metabolism than either alpha or delta cells (DiGruccio et al., 2016; Berthault et al., 2020).

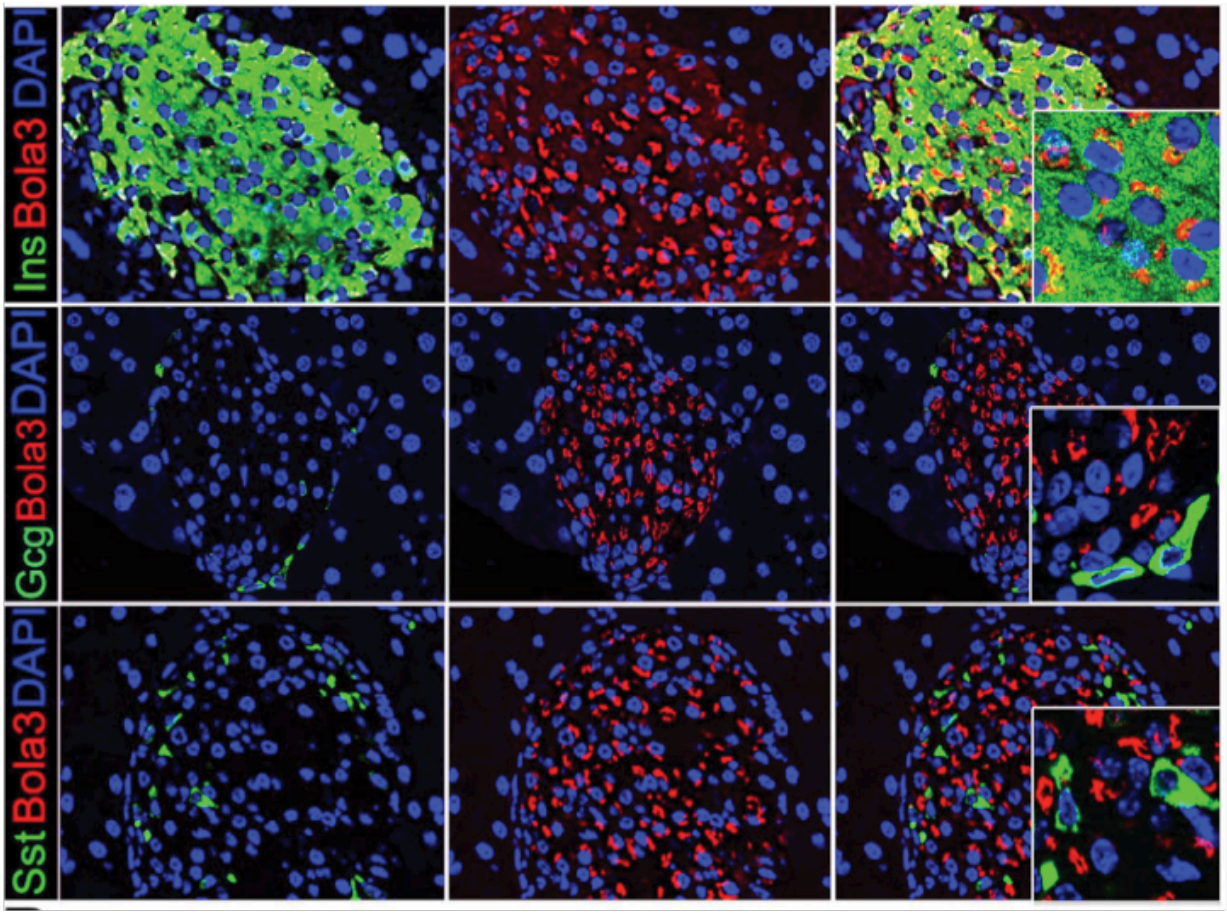

Figure 2-1. BOLA3 expression is most highly expressed in the beta cell in the adult murine pancreas. Adult, wild-type murine pancreata stained for BOLA3 (red) and DAPI (blue), and co-stained (green) for either insulin (Ins), glucagon (Gcg), or somatostatin (Sst).

Given these data, we sought to determine the role of *Bola3* in adult beta cell function using a tissue-specific, conditional mouse model of *Bola3* deficiency. *Bola3*$^{fl/fl}$ mice were bred with *Pdx1*$^{CreER/+}$ mice, in which the *Pdx1* promoter drives expression of the Cre recombinase-estrogen receptor fusion protein. *Pdx1* is ubiquitously expressed in the developing murine pancreas; however, its expression is largely restricted to beta

cells in the adult mouse. Administration of tamoxifen to *Pdx1*$^{CreER/+}$;*Bola3*$^{fl/fl}$ (*Bola3*^{KO}), *Pdx1*$^{CreER/+}$;*Bola3*$^{fl/+}$(*Bola3*^{HET}), and *Bola3*$^{fl/fl}$ or *Bola3*$^{fl/+}$ (*Bola3*^{WT}) mice at eight weeks of age via a five-day course of daily intraperitoneal injections therefore allowed us to interrogate *Bola3* in mature beta cells (Fig. 2-2A). Lipoylation of DLAT and DLST, the E2 subunits of PDH and αKGDH, is commonly used as a proxy for BOLA3 activity; islets isolated from *Bola3*^{KO} mice at eight months post-tamoxifen indeed displayed a significant and expected reduction of lipoylated DLAT and DLST (Fig. 2-2B,C), paired with a similarly significant reduction in *Bola3* transcript levels (Fig. 2-5A).

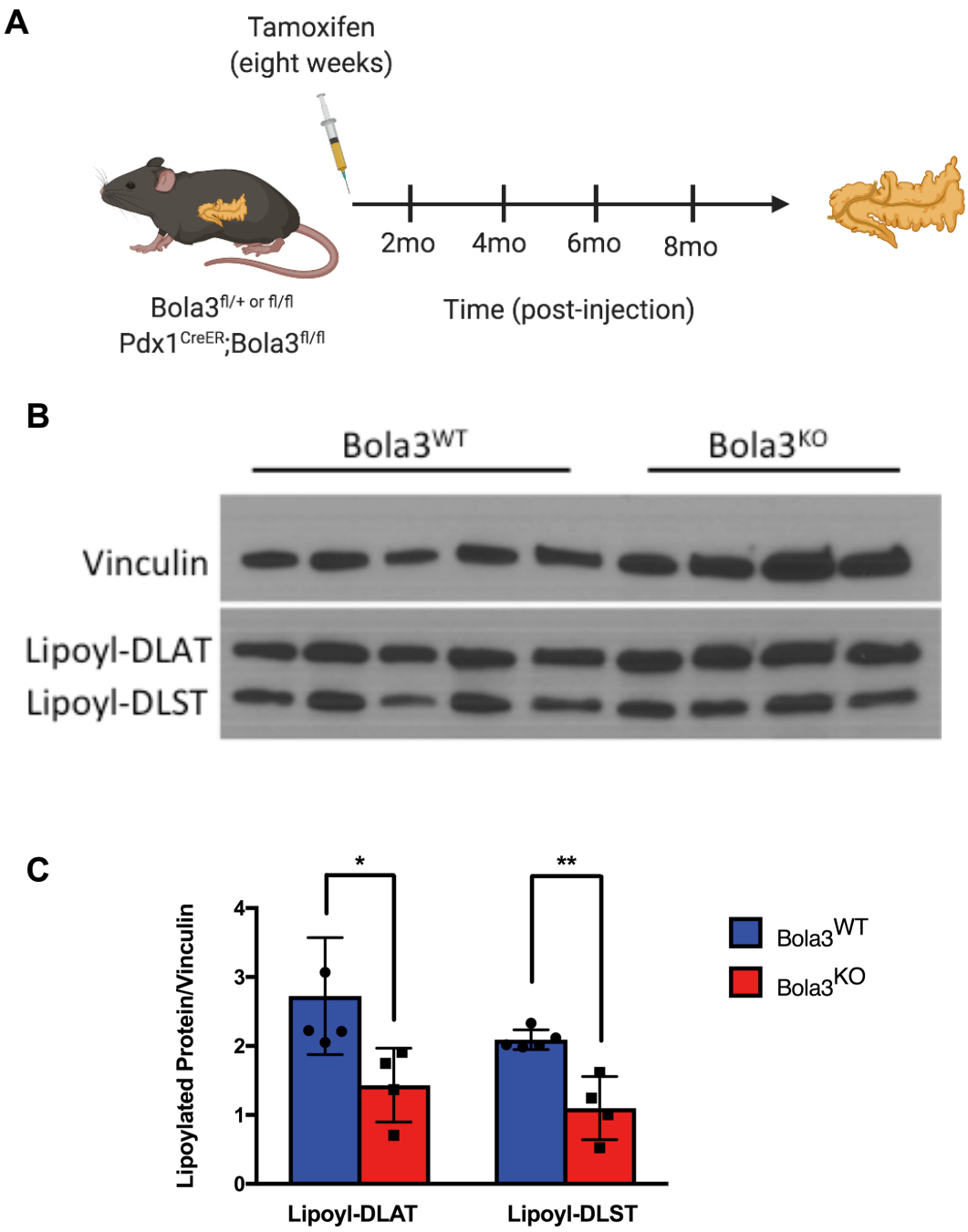

Figure 2-2. A mouse model of *Bola3* knockout. (A) Schematic indicating the experimental regimen of *Bola3*$^{fl/fl}$ or *Bola3*$^{fl/+}$ (*Bola3*^{WT}) and *Pdx1*$^{CreER/+}$;*Bola3*$^{fl/fl}$ (*Bola3*^{KO}) mice. (B) Western blot for lipoylation of downstream BOLA3 targets DLAT and DLST in *Bola3*^{WT} and *Bola3*^{KO} islets. (C) Quantification of (B).

Glucose tolerance tests were performed on *Bola3*^{KO} *Bola3*^{HET}, and *Bola3*^{WT} mice beginning one month post-tamoxifen to allow for sufficient recombination of the floxed

Bola3 allele and degradation of existing BOLA3 protein. Glucose tolerance tests were further performed at two, four, six, and eight months post-tamoxifen to track progressive defects in glucose homeostasis (Fig. 2-3A,B). *Bola3*^{KO} mice began exhibiting impaired glucose clearance compared to *Bola3*^{WT} mice four months after tamoxifen treatment, though they remained overall normoglycemic and responsive to glucose challenge. Within six months *Bola3*^{KO} mice demonstrated significant glucose intolerance, which worsened progressively to overt diabetes by eight months post-tamoxifen. No significant difference was observed between mice heterozygous for *Bola3*^{HET} and *Bola3*^{WT} mice until eight months post-tamoxifen, at which point *Bola3*^{HET} mice began to demonstrate an intermediate glucose intolerance phenotype. Though fasting blood glucose levels of *Bola3*^{KO} mice trend upwards, assessment of fasting blood glucose revealed no significant difference at six or eight months post-tamoxifen, despite the readily observable glucose intolerance of *Bola3*^{KO} animals (Fig. 2-3C). These data suggest that while *Bola3*^{KO} beta cells remain largely able to maintain basal glucose homeostasis, they are incapable of managing the increased cellular and respiratory demand induced by glucose challenge.

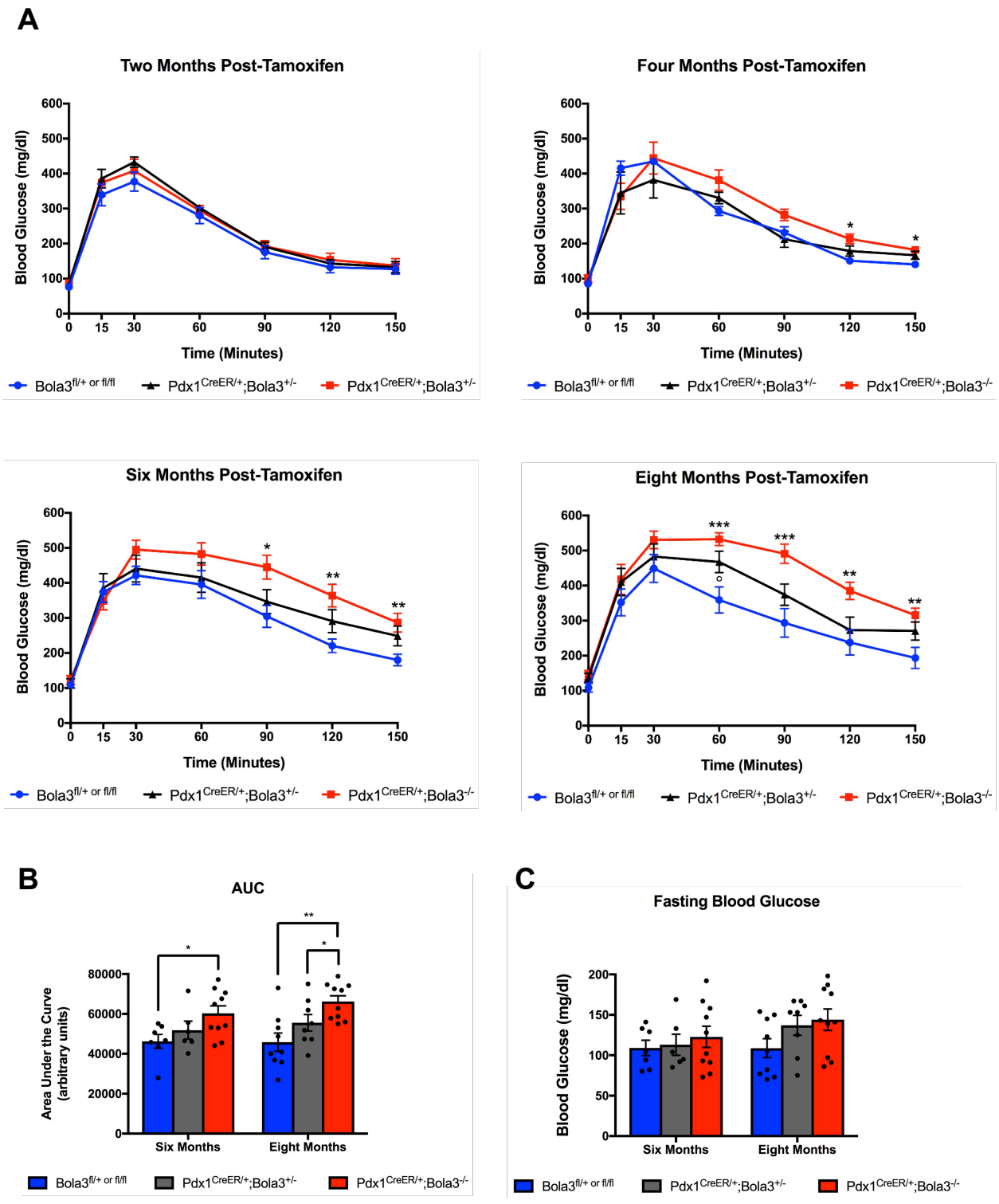

Figure 2-3. *Bola3*^{KO} mice exhibit dysfunctional glucose homeostasis *in vivo.* (A) Glucose tolerance tests performed on Bola3$^{fl/+}$ or $^{fl/fl}$, Pdx1^{CreER};Bola3$^{+/-}$, and Pdx1^{CreER};Bola3$^{-/-}$ mice at two, four, six, and eight months post-tamoxifen injection. (B) Area under the curve (AUC) quantification of (A). (C) Fasting blood glucose of Bola3$^{fl/+}$ or $^{fl/fl}$, Pdx1^{CreER};Bola3$^{+/-}$, and Pdx1^{CreER};Bola3$^{-/-}$ mice at six and eight months post-tamoxifen.

Intriguingly, our data demonstrate that *Bola3*^{KO} mice also exhibit elevated fasting serum insulin over time, a phenomenon that may underlie our observations regarding fasting blood glucose (Fig. 2-4A). This hyperinsulinemia is further accompanied by a lagging trend towards an increase in body, likely reflecting the known role of insulin as an adipogenic factor (Klemm et al., 2001; Zhang et al., 2009) (Fig. 2-4B). Observed impairments in glucose intolerance at six months post-tamoxifen in *Bola3*^{KO} mice precede significant increases in fasting serum insulin or body weight. Given this, and in combination with our data indicating that *Bola3*^{KO} and *Bola3*^{WT} mice demonstrate comparable insulin tolerance at six and eight months post-tamoxifen (Fig. 2-4C), we may discount the possibility that our phenotype is the result of acquired resistance to insulin. It may, however, arise as a secondary consequence.

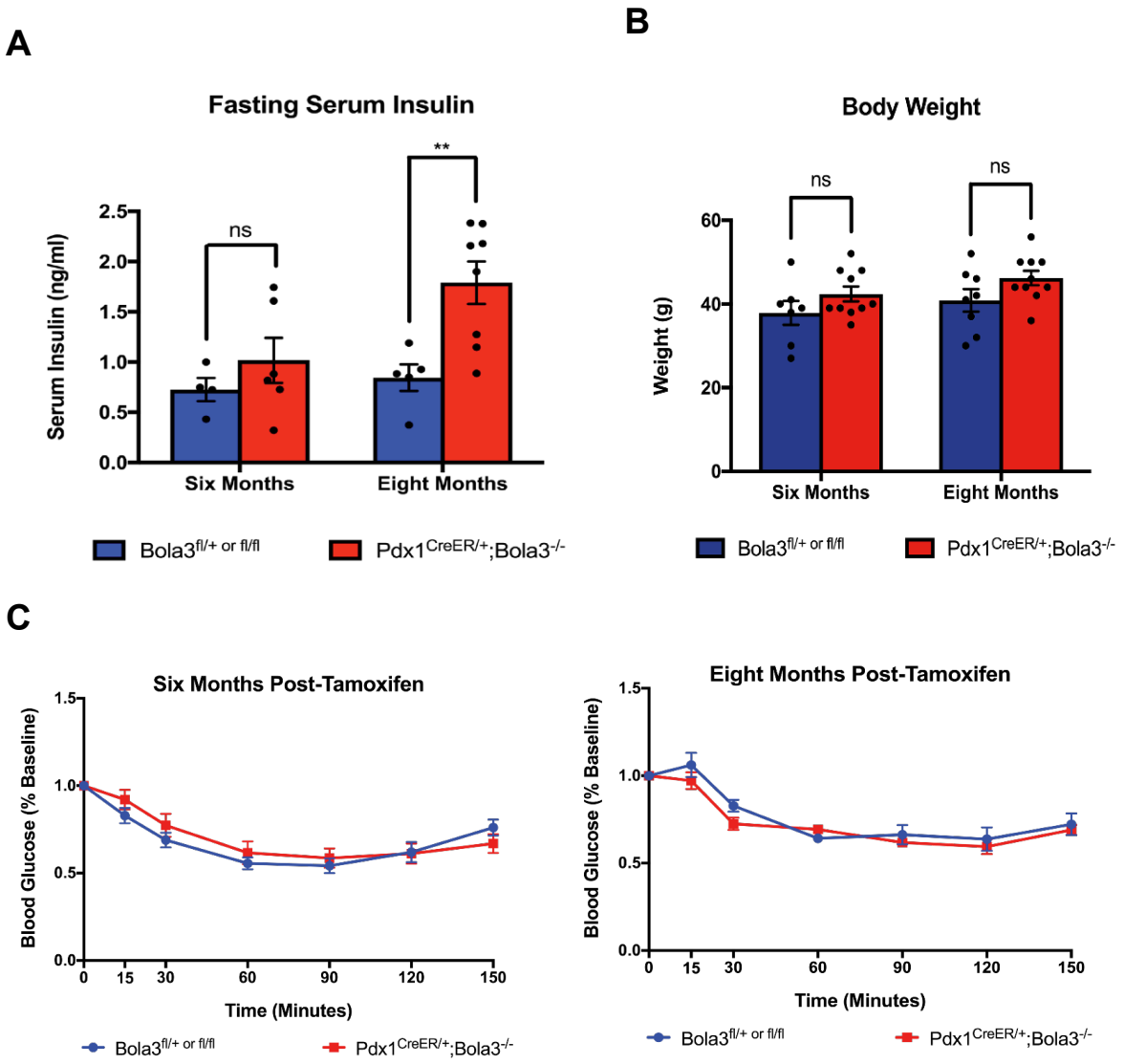

Figure 2-4. *Bola3^{KO} mice display late-stage fasting hyperinsulinemia and increased body weight without concurrent insulin resistance.* (A) Fasting serum insulin measurements of Bola3$^{fl/+ \text{ or } fl/fl}$ and Pdx1^{CreER};Bola3$^{-/-}$ mice six- and eight-months post-tamoxifen. (B) Body weight of Bola3$^{fl/+ \text{ or } fl/fl}$ and Pdx1^{CreER};Bola3$^{-/-}$ mice six- and eight-months post-tamoxifen. (C) Insulin tolerance tests performed on Bola3$^{fl/+ \text{ or } fl/fl}$ and Pdx1^{CreER};Bola3$^{-/-}$ mice at six- and eight-months post-tamoxifen (shown as percentage of baseline insulin).

Loss of Bola3 results in beta cell dedifferentiation

Increased basal insulin secretion is characteristic not only of insulin resistance, but also of beta cell immaturity (Jermendy et al., 2011; Blum et al., 2012; Puri et al., 2018). Indeed, beta cell dysfunction is frequently paired with erosion of the mature, terminally differentiated beta cell identity (Talchai et al., 2012; Puri et al., 2013; Wang et al., 2014; Puri et al., 2015). This process, known as beta cell dedifferentiation, is characterized by down-regulation of canonical beta cell genes, including *Pdx1*, *Nkx6.1*, *MafA*, and *Glut2,* frequently in conjunction with up-regulation of genes disallowed over the course of beta cell maturation (Fig. 2-5A). Quantitative PCR of *Bola3*^{KO} and *Bola3*^{WT} islets isolated eight months post-tamoxifen revealed that *Bola3*^{KO} and *Bola3*^{WT} islets equivalently express the *Ins1* and *Ins2* transcripts. However, *Bola3*^{KO} islets showed significant reductions in *Pdx1*, *Nkx6.1*, *MafA*, and *Glut2* (Fig. 2-5B).

In accordance with these findings, immunofluorescent staining of *Bola3*^{KO} and *Bola*^{WT} pancreata revealed subtle differences in PDX1 and NKX6.1 paired with a drastic reduction in both membranous GLUT2 and the pool of cytoplasmic GLUT2 reserved for trafficking to the membrane (Fig. 2-5C). Further immunofluorescent assessment of *Bola3*^{KO} islets revealed diminished PC1/3, a prohormone convertase critical for processing the precursor molecule proinsulin, concurrent with a striking increase in the islet proinsulin:insulin ratio (Fig. 2-5D).

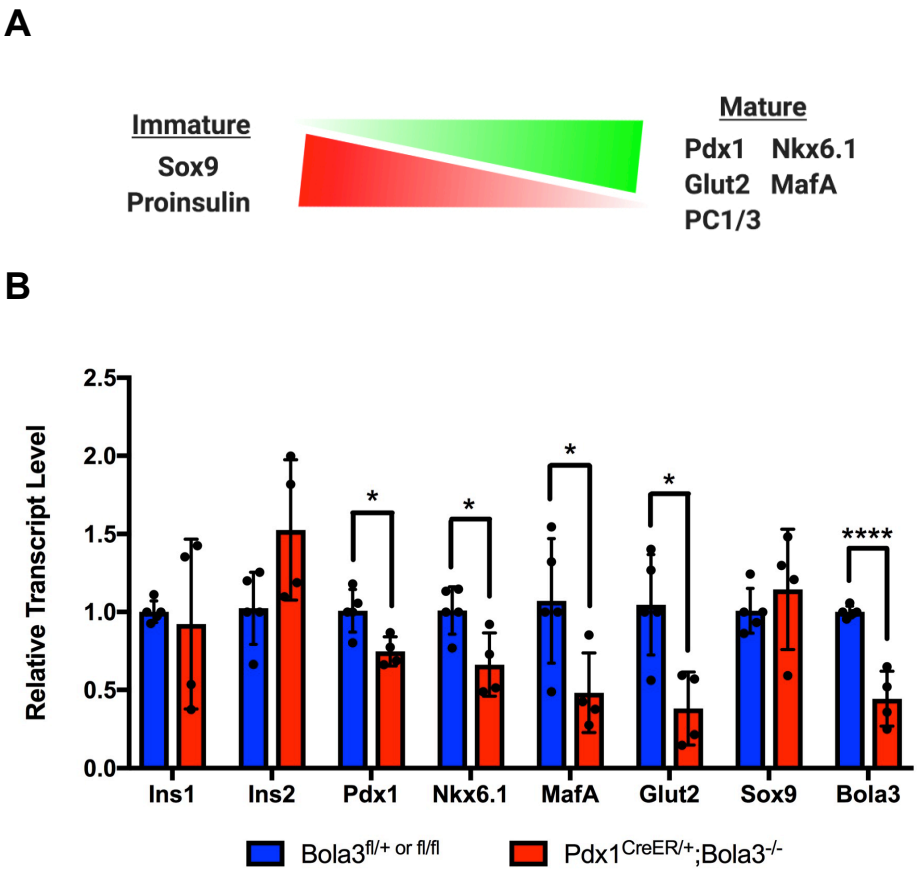

Figure 2-5. Loss of Bola3 results in downregulation of canonical beta cell markers. (A) Canonical markers of immature and mature beta cells. (B) qPCR analysis of beta cell identity genes in islets isolated from *Bola3*$^{fl/+ \text{ or}}$ or *Pdx1*$^{CreER/+}$;*Bola3*$^{-/-}$ mice.

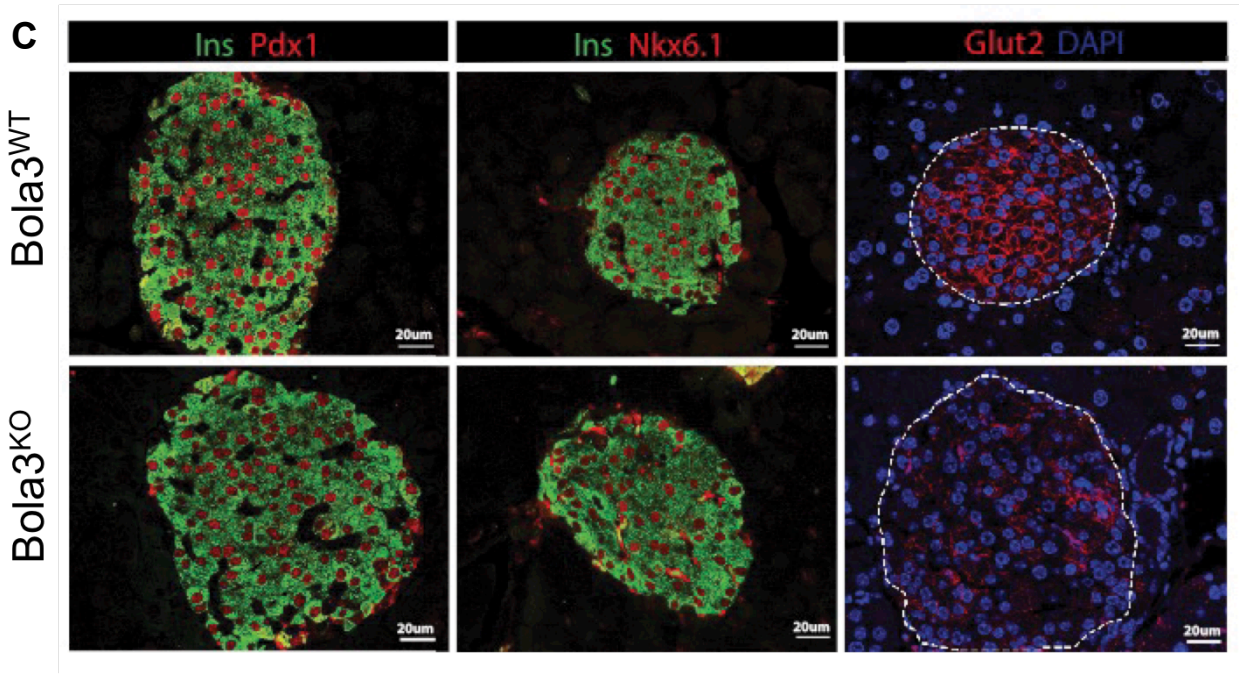

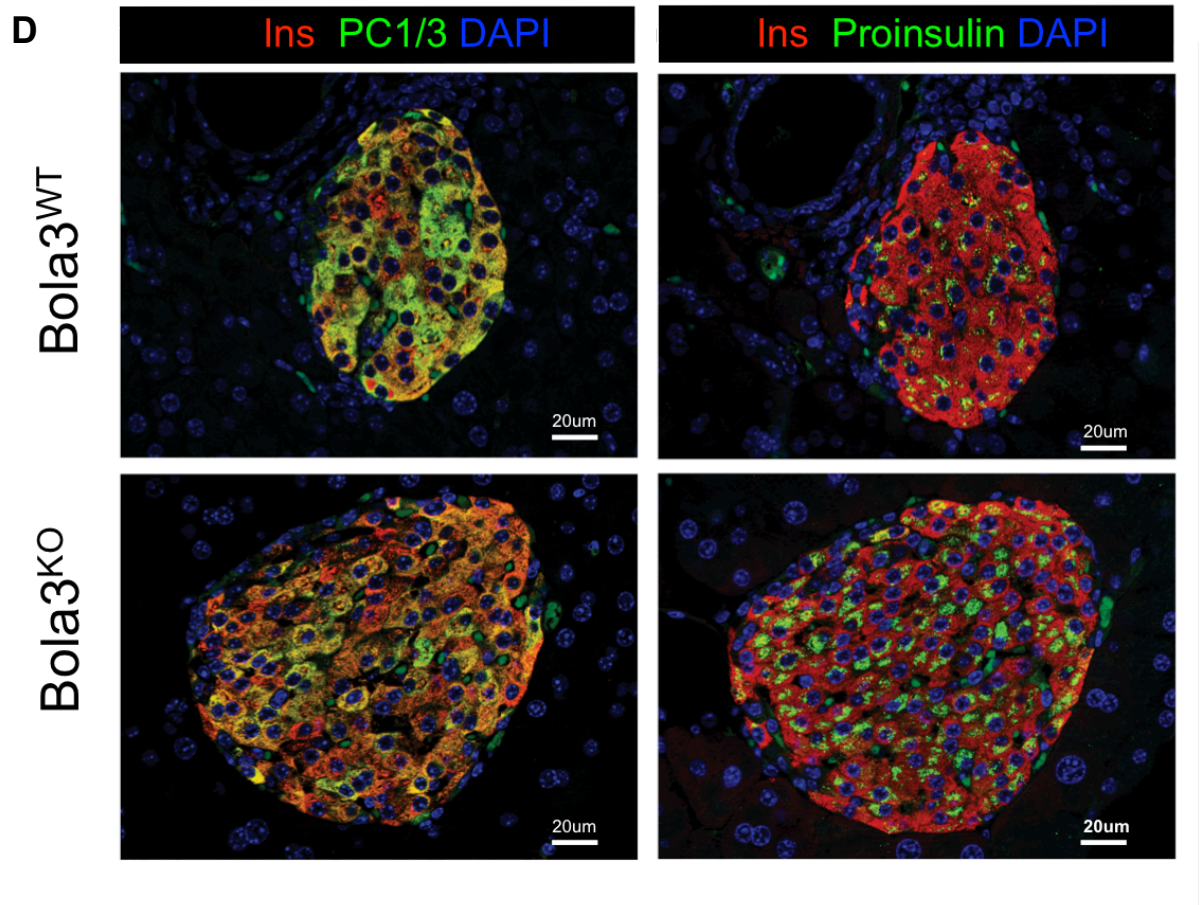

Figure 2-5 (cont'd). Loss of Bola3 results in downregulation of canonical beta cell markers. *Bola3*^{WT} and *Bola3*^{KO} pancreata stained for PDX1, NKX6.1, or GLUT2 (red, C) and PC1/3 or proinsulin (green, D).

Bola3^{WT} islets possess a limited number of alpha cells localized to the islet periphery, as has been previous described in examinations of murine islet architecture (Kim et al., 2009; Steiner et al., 2010) (Fig. 2-6, top panel). Intriguingly, however *Bola3*^{KO} pancreata contain both islets similar to those found in *Bola3*^{WT} pancreata and islets exhibiting perturbed cellular composition and distribution (Fig. 2-6, bottom panel). These include large islets with peripheral and "demarcating" alpha cells (Fig. 2-6, bottom middle) and small islets demonstrating both a greatly increased alpha:beta cell ratio and alpha cells fully distributed throughout the islet (Fig. 2-6, bottom right). The former suggests either cellular migration into the islet interior or islet fusion; the latter may indicate the collapse of the islet architecture, possibly due to beta cell death.

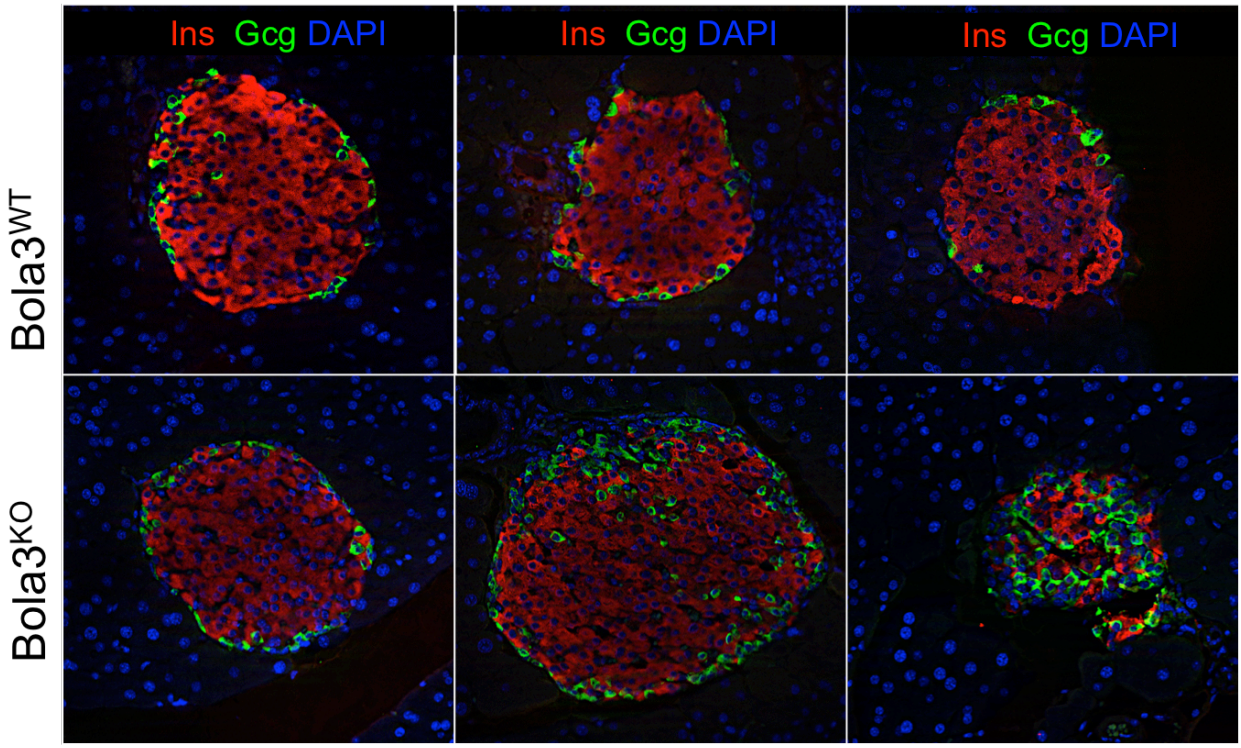

Figure 2-6. Altered alpha cell number and distribution in *Bola3*^{KO} islets. Immunofluorescent staining of *Bola3*^{WT} and *Bola3*^{KO} pancreata for insulin (Ins, red), glucagon (Gcg, green) and DAPI (blue).

Islets deficient in Bola3 demonstrate mitochondrial fragility and decreased cellular respiration

We next sought to interrogate the metabolic profile and mitochondrial function of isolated *Bola3*-deficient islets using Seahorse XF analysis, which measures oxygen consumption rate (OCR), an indicator of mitochondrial oxidative phosphorylation. Assessment of the oxygen consumption rate (OCR) as a percentage of basal OCR of *Bola3*^{KO} and *Bola*$^{\beta WT}$ islets indicates that *Bola3*^{KO} islets are capable of mounting a respiratory response with similar dynamics as *Bola3*^{WT} islets in response to glucose stimulation (Fig. 2-7A). Interestingly, normalizing oxygen consumption rate to total insulin content indicates that *Bola3*^{KO} islets broadly consume less oxygen than *Bola3*^{WT} islets, thereby suggesting that *Bola3*^{KO} islets engage less extensively in mitochondrial respiration upon glucose challenge (Fig. 2-7B). We previously demonstrated that *Bola3*^{KO} islets exhibit only partial knockout of *Bola3* (Fig. 2-5B). Our Seahorse data suggest that, rather than a uniform decrease in *Bola3* expression, there may exist two distinct subcategories of beta cells within *Bola3*^{KO} islets: *Bola3*^{high} beta cells capable of mounting a respiratory response, and *Bola3*^{low} beta cells unable to do so (Fig. 2-7C). This may account for the observed discrepancy between the baselined and total insulin-normalized *Bola3*^{KO} and *Bola3*^{WT} data. *Bola3*^{KO} islets demonstrate increased sensitivity to the mitochondrial respiratory chain complex inhibitors oligomycin, antimycin A, and rotenone than *Bola3*^{WT} islets (Fig. 2-7D). This increased susceptibility of *Bola3*^{KO} islets to mitochondrial poisons suggests that loss of *Bola3* within *Bola3*^{KO} islets, whether uniformly or in a select subpopulation of *Bola3*^{low} beta cells, constitutes a metabolic

insult sufficient to affect other forms of cellular respiration and further diminish the ability of the beta cell to withstand metabolic stressors concurrent with glucose challenge.

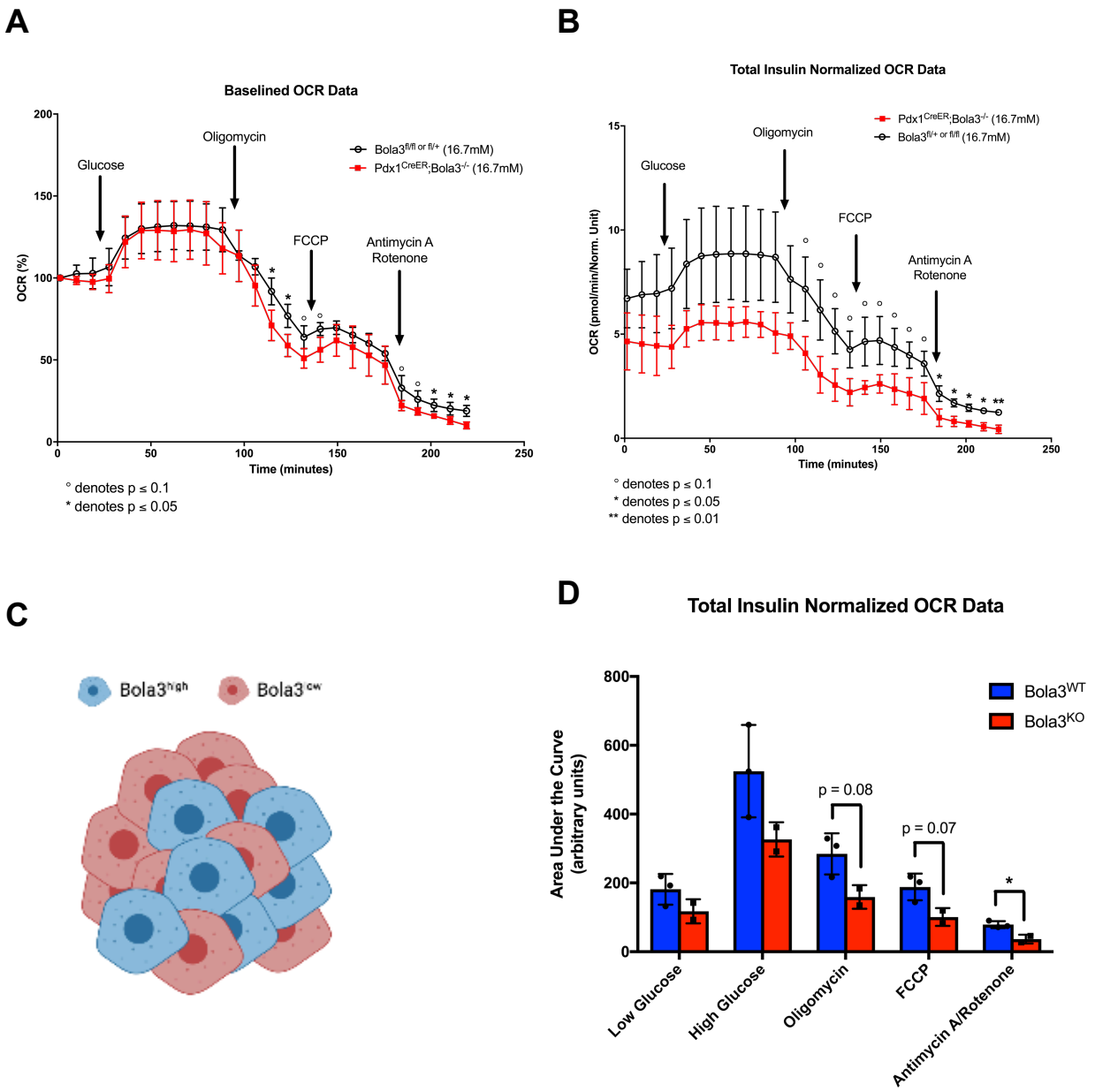

Figure 2-7. Decreased mitochondrial and non-mitochondrial respiration in *Bola3*-deficient islets. (A) Oxygen consumption rate (OCR) as a percentage of baseline oxygen consumption. (B) Total insulin-normalized OCR. (C) *Bola3*^{KO} islets as a mixed population of *Bola3*^{high} and *Bola3*^{low} beta cells. (D) Total insulin-normalized OCR represented as AUC during each discrete phase of Seahorse XF analysis.

Discussion:

Our study reveals a role for the mitochondrial Fe-S cluster transport protein BOLA3 in the beta cell. *Bola3* knockout in the adult murine beta cell results in the progressive development of *in vivo* glucose intolerance and occurs in the absence of concurrent insulin resistance. This perturbation in global glucose homeostasis, the gradual nature of which recapitulates the pathogenesis of type 2 diabetes, is further paired with late-stage hyperinsulinemia and weight gain. It should be noted, however, that prior research has found that tamoxifen, when administered at sufficiently high dosages, is capable of inducing hypothalamic recombination in the *Pdx1*$^{CreER/+}$ mouse line (Wicksteed et al., 2010). The hypothalamus has been found to play a role in glucose sensing and insulin secretion (Osundiji et al., 2012; Routh et al., 2014; Hirschberg et al., 2020). For that reason, while these experiments utilized a tamoxifen dosage situated at the lower range of those tested, it remains possible that Bola3 loss within the hypothalamus contributed to our observations.

Increased basal insulin secretion is a hallmark of beta cell immaturity (Jermendy et al., 2011; Blum et al., 2012; Puri et al., 2018). Indeed, our data indicate that *Bola3* knockout results in the perturbation of canonical mature beta cell markers in a manner consistent with cellular de-differentiation. De-differentiation is increasingly thought to function as a protective mechanism enacted in response to various physiological stressors to allow the beta cell to ensure its own survival (Talchai et al., 2012; Cerf, 2013). Interestingly, it has been shown that ablation of either LIAS or aKGDH leads to activation of the cellular hypoxia response under normoxic conditions. This occurs through the buildup of the metabolite L-hydroxyglutarate, which is generated when a-ketoglutarate cannot be converted to succinyl-CoA by aKGDH. L-hydroxyglutarate

inhibits the prolyl hydroxylase (PHD) domain of HIF transcription factors, thereby stabilizing them even in the presence of oxygen (Burr et al., 2016). Our prior research has demonstrated that non-physiological induction of HIF1a in the beta cell has deleterious effects on both beta cell function and beta cell identity (Puri et al., 2009; Puri et al., 2013). Given the role of BOLA3 in regulating LIAS and, consequently, αKGDH, it is possible that the beta cell de-differentiation observed in *Bola3*^{KO} mice is linked to inappropriate activation of the cellular hypoxia response.

BOLA3 mediates multiple aspects of aerobic respiration, including the TCA cycle and oxidative phosphorylation. Indeed, loss of *Bola3* diminished the mitochondrial respiratory capacity and increased the sensitivity to mitochondrial poisons of in *Bola3*^{KO} islets. It should be noted that *Bola3*-deficient MMDS patient tissues retain a low level of mitochondrial respiratory chain complex activity. In conjunction with our data demonstrating significant, though incomplete ablation of *Bola3* in *Bola3*^{KO} islets, this may partially underlie the measure of mitochondrial function still present in *Bola3*^{KO} islets. As previously discussed, we additionally postulate that the ability of *Bola3*^{KO} islets to mount a respiratory response with a dynamic similar to that of *Bola*^{WT} islets may result from the presence of two distinct populations of *Bola3*^{high} and *Bola3*^{low} beta cells, as has been observed in BOLA3^{KO} eBCs.

CHAPTER 3.

Recombinant murine BOLA3 protein as a novel beta cell secretagogue

Introduction:

Though BOLA3 canonically functions within the mitochondria, it has previously been shown that Cos-7 monkey kidney fibroblasts-like cells transiently transfected with recombinant plasmids are capable of secreting BOLA proteins (Zhou et al., 2008). Importantly, recent proteomic analysis has identified BOLA3 as a member of the human brown adipocyte secretome (Kajimura, unpublished). Cultured primary adipocytes transfected with an adenoviral vector carrying a *Bola3* expression construct secrete BOLA3 into culture media; tail-vein injection of this vector into diet-induced obese mice resulted in circulating serum BOLA3 and a significant improvement in glucose tolerance. Taken together, these data have critical biological implications: first, that BOLA3 may be secreted by human cells, particularly adipocytes, under certain physiological conditions. Second, that secreted BOLA3 may play a role in regulating glucose homeostasis. Given the extensive intercellular communication between adipocytes and beta cells through various signaling molecules, including secreted proteins, we sought to determine the effect of exposing beta cells to exogenous BOLA3.

Results:

Recombinant murine BOLA3 protein (rBOLA3) was produced via transient transfection of mammalian HEK293 cells. This vector carried the murine BOLA3 coding sequence appended to a C-terminal FLAG tag for the purpose of purification.

In vitro static glucose-stimulated insulin secretion assays were performed with isolated murine islets. After equilibration with low levels of glucose (2.8mM), islets were either kept under low glucose conditions or switched to high glucose conditions (16.7mM), with or without rBOLA3 for one hour to recapitulate exposure to secreted BOLA3. Promisingly, islets treated with rBOLA3 demonstrated significantly increased stimulation indices when compared to untreated control islets (Fig. 3-1A). This functional improvement was evident exclusively at 16.7mM glucose; treatment with rBOLA3 was ineffective at 2.8mM glucose. Furthermore, islets were found to respond to rBOLA3 treatment in a dose-dependent manner, though the phenomenon became diminished at higher rBOLA3 concentrations (Fig. 3-1B). Notably, treatment of isolated human islets with rBOLA3 recapitulated the improvement in stimulation indices observed upon treatment of isolated murine islets (Fig. 3-2).

A

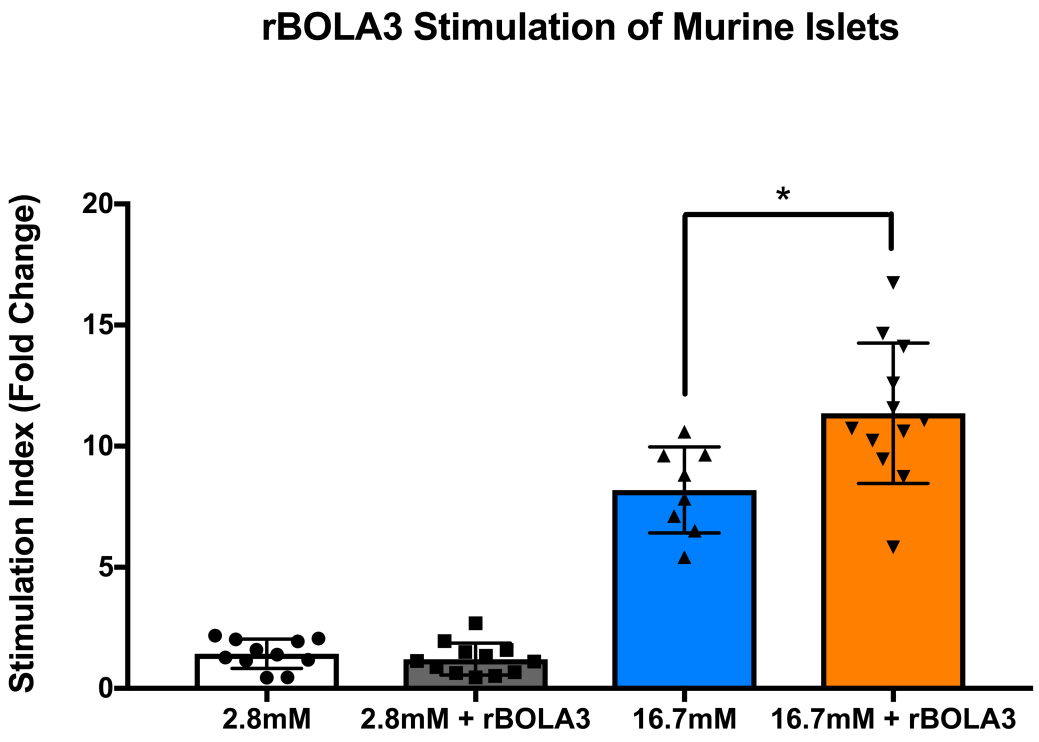

B

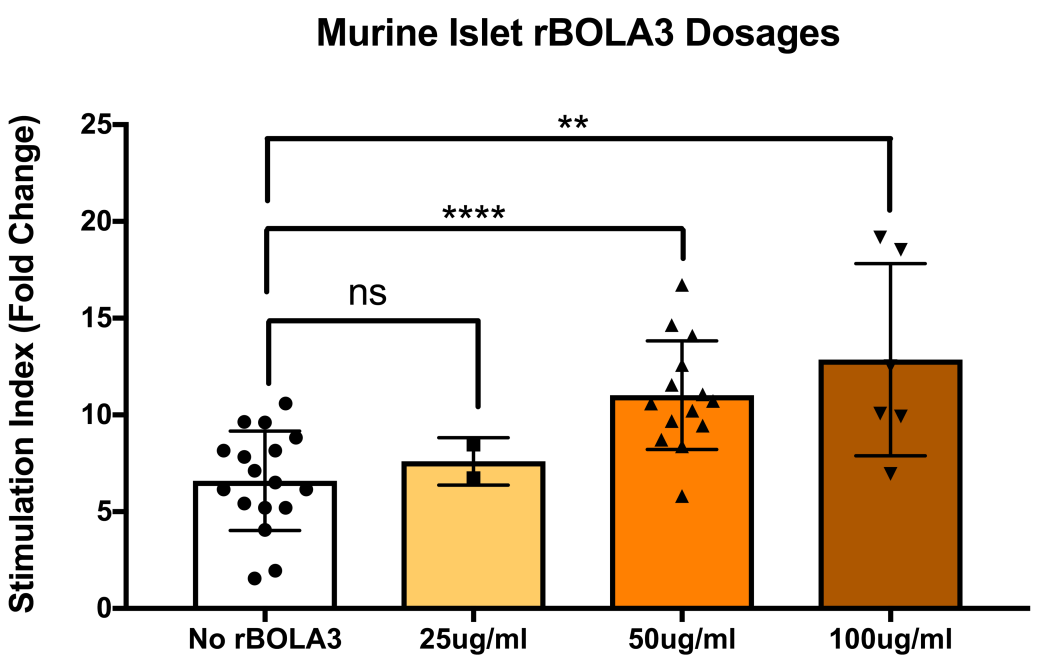

Figure 3-1. Recombinant BOLA3 protein augments murine islet insulin secretion in a dose-dependent manner. (A) Murine islets cultured at either low or high glucose for one hour, with or without rBOLA3 (50ug/ml). (B) Murine islets cultured at high glucose with 25ug/ml, 50ug/ml, or 100ug/ml of rBOLA3.

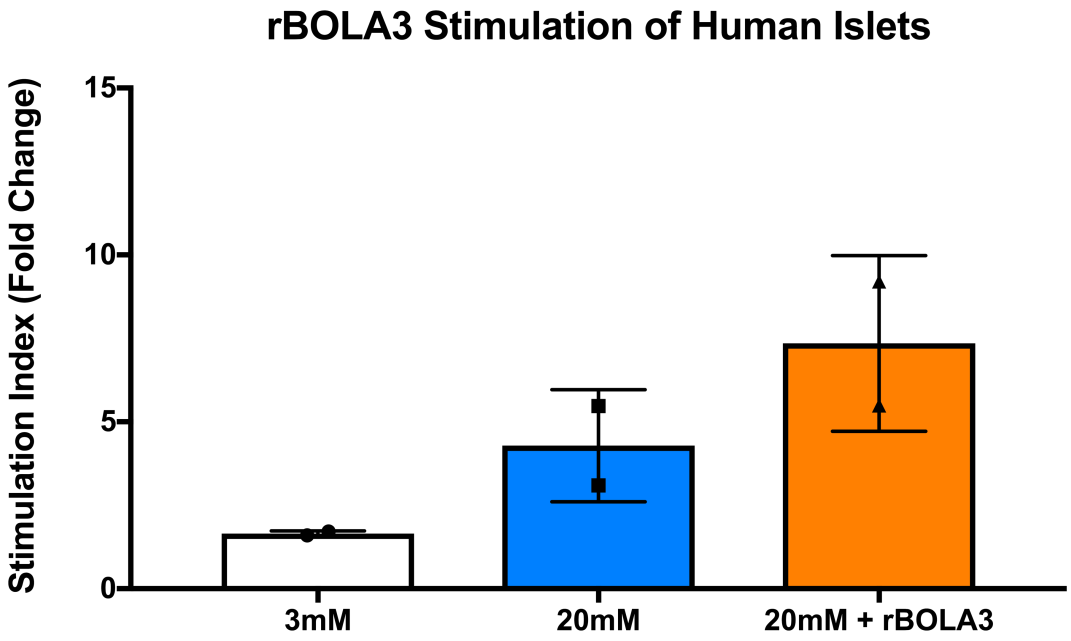

Figure 3-2. Recombinant BOLA3 protein augments human islet insulin secretion. Human islets cultured at either low or high glucose for one hour, with or without rBOLA3 (50ug/ml).

Discussion:

It has previously been determined that intraperitoneal injection of rBOLA3 into diet-induced obese mice improves glucose tolerance (Kajimura, unpublished). However, glucose homeostasis is controlled by multiple organ systems, including both the islet and various peripheral tissues. For this reason, this observed improvement in global glucose tolerance upon treatment with rBOLA3 could not be taken as conclusive evidence that rBOLA3 affects beta cell function. Our results demonstrate that exposure to exogenous rBOLA3 specifically improves beta cell function, as defined as glucose-stimulated insulin secretion, *in vitro*, thereby establishing a role for BOLA3 as a novel beta cell secretagogue.

These data further suggest that rBOLA3 is not only capable of augmenting beta cell function, but that it does so in a glucose-dependent manner. Islets treated with

rBOLA3 demonstrated modulated insulin secretion exclusively upon exposure to stimulatory (16.7mM or 20mM) glucose concentrations; no difference between treated and untreated islets was observed at sub-stimulatory (2.8mM or 3mM) glucose concentrations. The fact that rBOLA3 is sensitive to glucose concentration sets it apart from other anti-diabetics, such as sulfonylureas, a class of therapeutic agents commonly used to treat type 2 diabetes. Sulfonylureas, as K_{ATP} channel blockers, act independently of blood glucose levels, causing beta cells to continuously and indiscriminately release insulin.

Because this marks the first evidence that the rBOLA3 protein acts exogenously as an insulin secretagogue, many critical questions remain. One of the most pressing is how rBOLA3 interacts with the beta cell at the cell surface in order to alter GSIS. The mechanics of GSIS are largely intracellular, and we have excluded the possibility of action on K_{ATP} and Ca^{2+} channels, two of the only components of the GSIS machinery readily accessible to exogenous proteins. Therefore, it is plausible that rBOLA3 is internalized by the beta cell, potentially through the process of receptor-mediated endocytosis. Alternately, exogenous rBOLA3 may remain extracellular and trigger a downstream signaling cascade.

It should be noted that further validation of these novel results is highly advisable. Exome sequencing of two siblings with MMDS identified the same c.200T>A homozygous point mutation, resulting in a p.Ile67Asn substitution, for which both parents were heterozygous carriers (Haack et al., 2013). Given this, we have designed a vector harboring the coding sequence for the identified mutant BOLA3 variant to be utilized for the concurrent production and testing of functional and nonfunctional rBOLA3.

CHAPTER 4.

The role of BOLA3 in the human beta cell

Introduction:

Reflecting its role as a regulator of mitochondrial metabolism, the *Bola3* transcript and protein are found to varying degrees across human tissues, including the pancreas (Uhlén et al., 2015), though data establishing cell-type specificity is limited. Prior studies have interrogated the role of BOLA3 in the human brain, heart, and brown fat (Baker, II, et al., 2014; Imai-Okazaki et al., 2019; Tajima et al., 2019; Bai et al., 2021). We therefore sought to rectify the dearth of research devoted to the expression and role of BOLA3 in the human islet and beta cells.

Given the scarcity and limitations of human pancreata and islets, our lab has devoted significant efforts over the last decade in establishing a platform to interrogate beta cell disease in human cells. Using a precise, sequential recapitulation of developmental principles, we can now generate beta cells from human stem cells in a dish. Our enriched beta clusters, or eBCs, are the product of a novel protocol developed by our lab for the purpose of driving maturation of human embryonic stem cell-derived beta cells, thereby allowing them to better recapitulate those found in human islets (Nair et al., 2019). Following a 20-day differentiation protocol, our Ins-GFP human embryonic stem cell line can give rise to beta-like cells that display widespread GFP expression (controlled by the endogenous insulin promoter) with >75% C-peptide positivity. Isolation of GFP+ cells via FACS followed by reaggregation of the purified cells produces clusters comprised of >90% C-peptide+, mono-hormonal cells. Our data demonstrate that eBCs include functional beta cells that strongly resemble human islets

in terms of transcriptional profile, dynamic GSIS, Ca^{2+} signaling, and Seahorse analyses. Of note, eBCs are capable of rapidly regulating glucose levels upon transplantation in diabetic mice, further supporting the notion that their functional properties closely resemble those of human islets. Utilization of these eBCs therefore allows us to investigate BOLA3 expression and function in the human beta cell *in vitro* and with a model system that confers significant biological relevance.

Results:

Correlation between BOLA3 and cellular maturity in human beta cells

Immunofluorescent staining of human pancreata indicates strong BOLA3 expression in the endocrine compartment, predominately localizing to insulin+ beta cells, though expression was also observed in somatostatin+ delta cells (Fig. 4-1A). To further probe the role of BOLA3 in the human beta cell *in vitro* we utilized eBCs, which strongly recapitulate the function and mitochondrial metabolism of human islets. Immature, beta-like clusters contain less BOLA3 than eBCs (Fig. 4-1), suggesting that BOLA3 levels correlate with cellular maturity in the human beta cell.

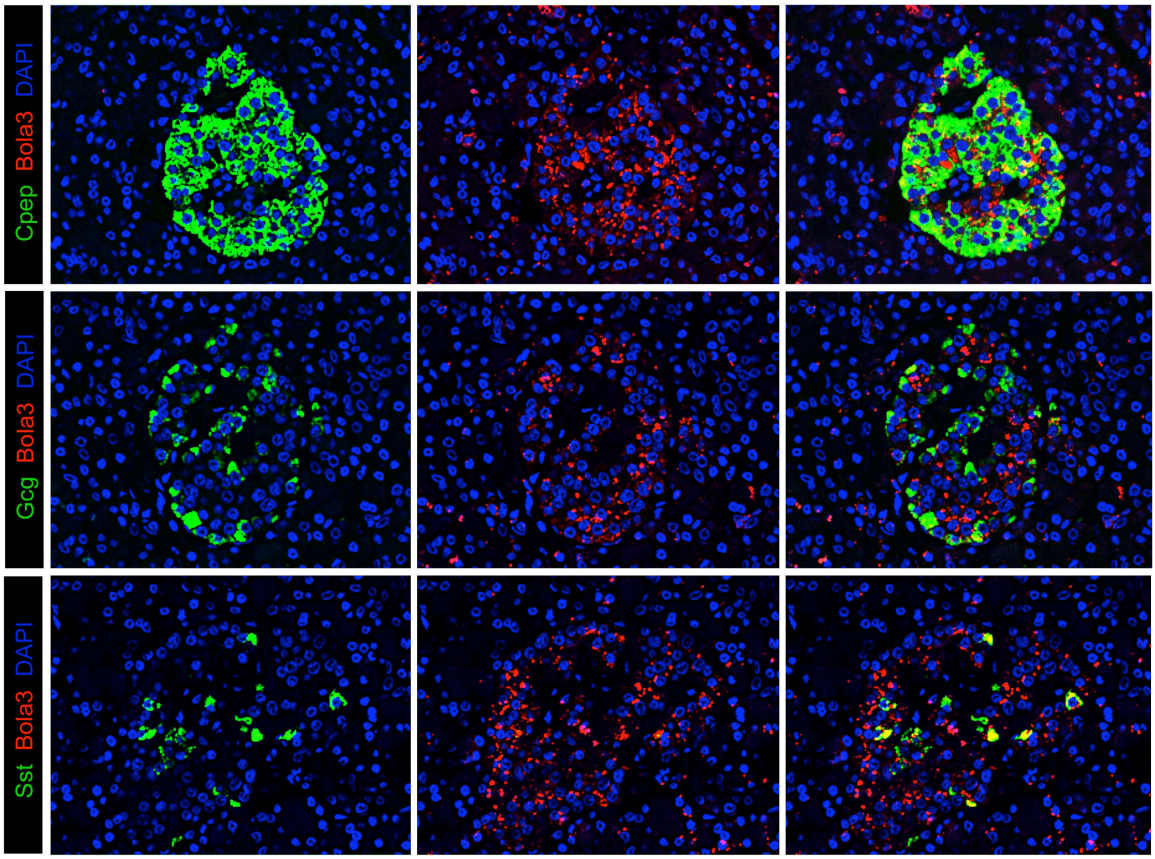

Figure 4-1. BOLA3 localizes to endocrine cells within the human pancreas. Adult human pancreata stained for BOLA3 (red) and DAPI (blue), and co-stained (green) for either insulin (Ins), glucagon (Gcg), or somatostatin (Sst).

A

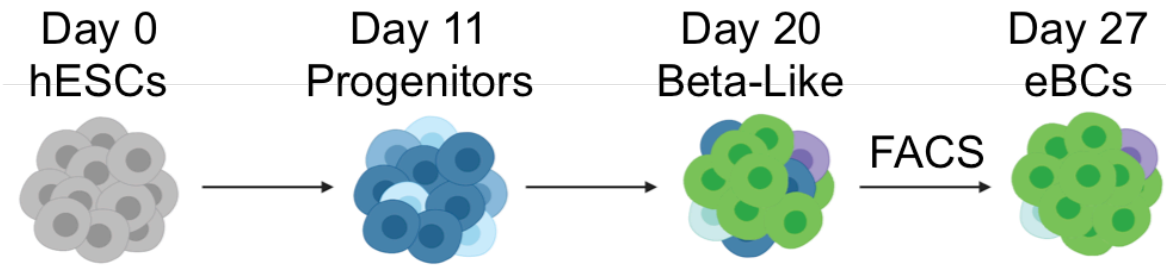

B

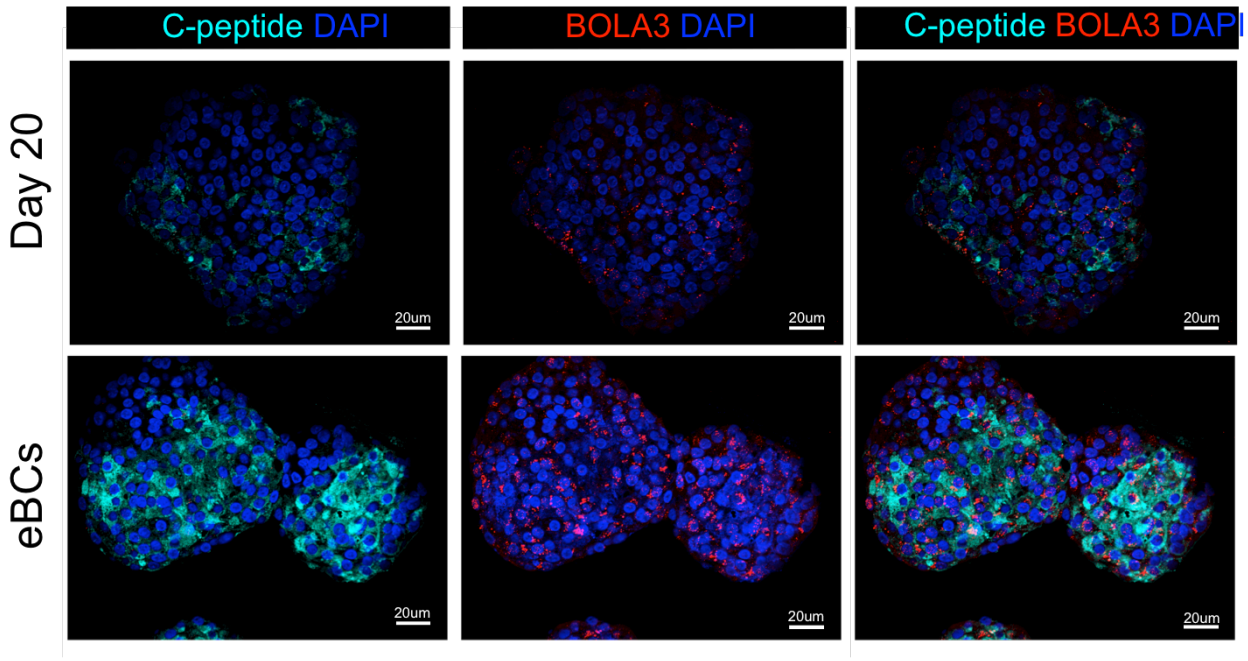

Figure 4-2. Enriched beta clusters possess contain more BOLA3 than immature, beta-like clusters. (A) Directed differentiation of human embryonic stem cells (day 0) into pancreatic progenitors (day 11), immature, beta-like cells (day 20), and eBCs (day 27, post-FACS). (B) Day 20 clusters and eBCs stained for C-peptide (cyan), BOLA3 (red), and DAPI (blue).

To gain further insight into the genes and pathways that influence metabolic maturation of eBCs, we examined RNA sequencing data previously generated by our lab to compare immature, beta-like clusters to eBCs (Fig. 4-3A). In accordance with our protein data, *Bola3* appeared to be upregulated in eBCs. As anticipated based on previous studies demonstrating enhanced mitochondrial metabolism in eBCs, various protein components of mitochondrial respiratory chain (MRC) complexes I, II, and III were upregulated in eBCs. Intriguingly, though, many genes associated with the aerobic respiration and the TCA cycle, including those encoding for downstream BOLA3 targets LIAS, DLAT, and DLST, were expressed at comparable levels between immature, beta-like clusters and eBCs. These data suggest the maturation of mitochondrial metabolism in eBCs may be characterized and driven by altered expression of a subset of critical genes, including BOLA3.

To probe the validity of these findings in the context of human beta cells, we analyzed publicly available RNA sequencing data comparing adult (30 year-old) and juvenile (3 year-old) beta cells (Fig. 4-3B). While we found multiple commonalities between the datasets, including the upregulation of genes encoding for various MRC complex subunits, we also observed several intriguing differences. Both BOLA3 and NFU1 are upregulated upon the progression of Day 20 spheres into eBCs; however, BOLA3 is the only Fe-S cluster transport protein significantly upregulated in adult human beta cells versus juvenile beta cells. These data further support the notion that *BOLA3* expression is correlated with maturation of the beta cell.

A

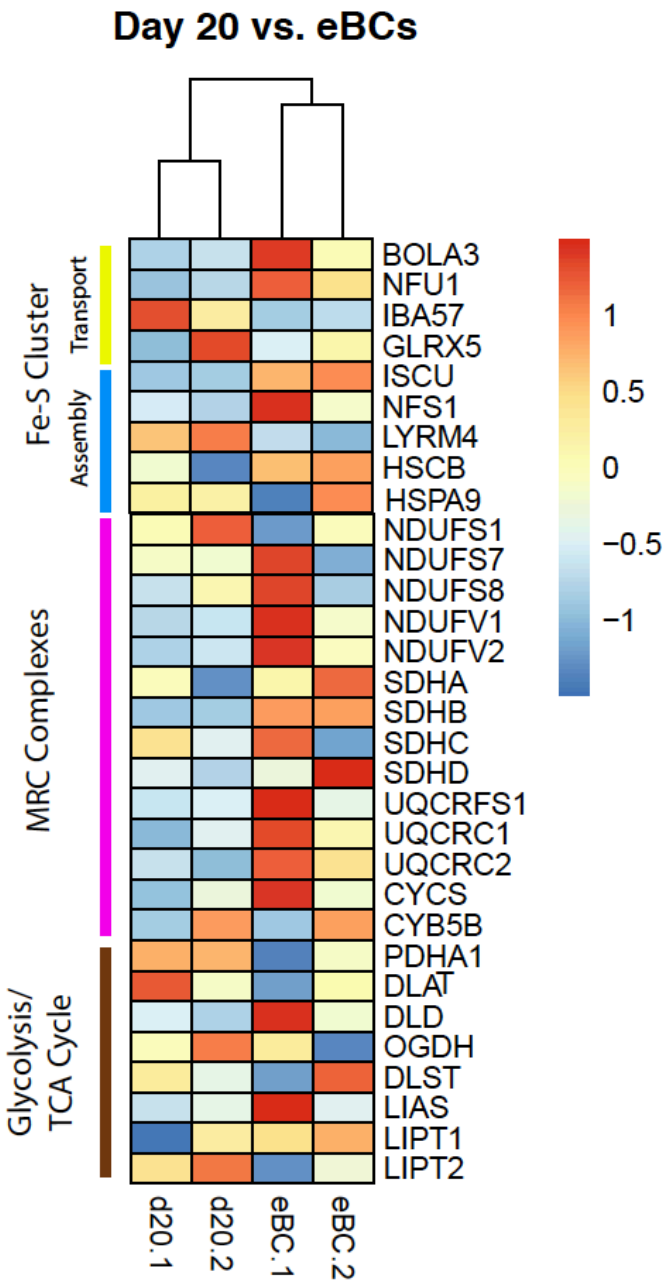

Figure 4-3. Upregulation of iron-sulfur cluster and mitochondrial respiratory chain complex genes correlates with cellular maturity. Heat-maps depicting RNA sequencing data of genes relevant to iron-sulfur cluster assembly and transport, mitochondrial respiratory chain complexes, and glycolysis and the TCA cycle. Gene expression is compared between immature, beta like cells (Day 20) and eBCs (A) or mature (30 year-old) and juvenile (3 year-old) beta cells (B).

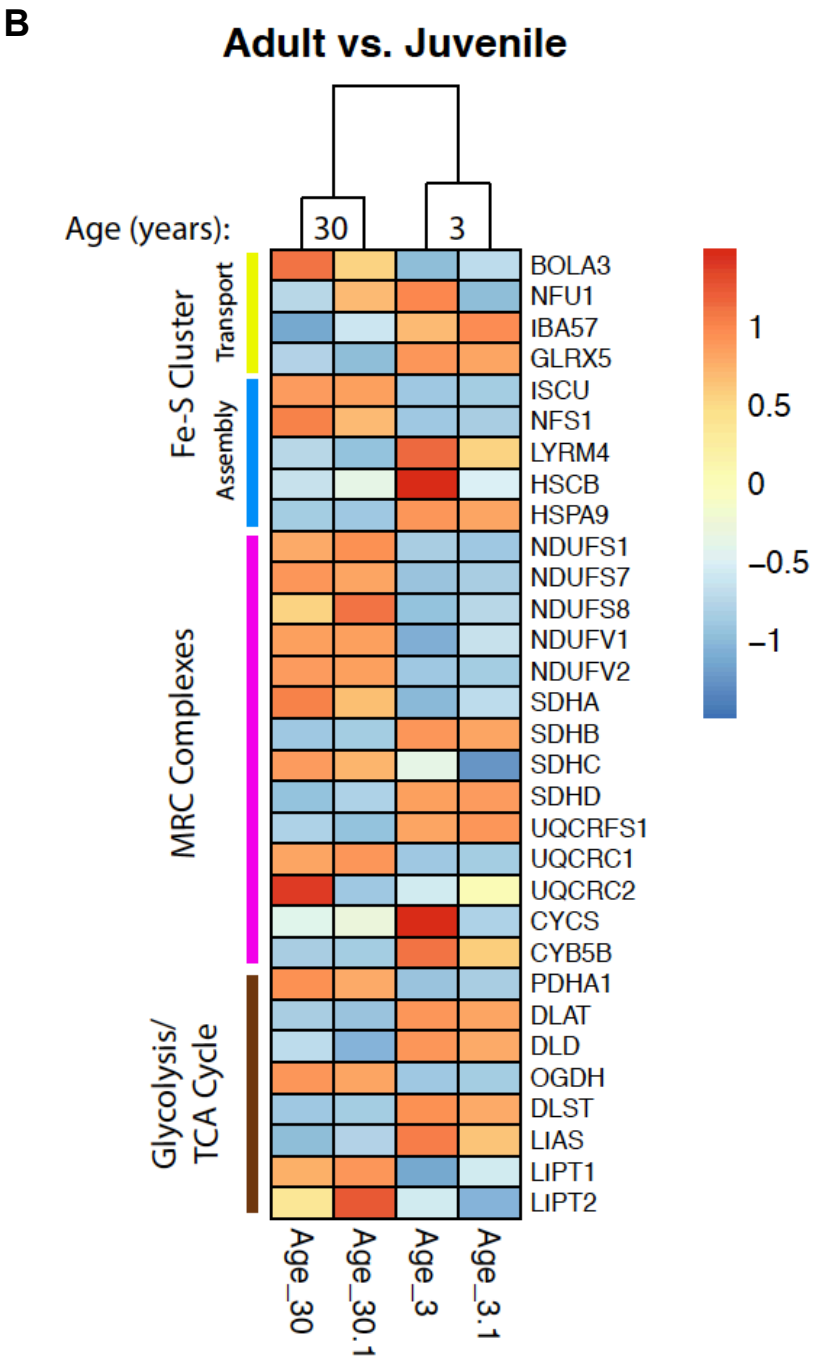

Figure 4-3 (cont'd).

CRISPR-Cas9 ablation of Bola3 in human stem cell-derived beta cells

Given its expression in the human beta cell, we sought to investigate the effect of abolishing BOLA3 *in vitro* with our hESC-derived beta cell system. To that end, we used TALEN targeting to generate an inducible CRISPR-Cas9 BOLA3 hESC line ($BOLA3^{KO}$). Two hAAVS1-targeted vectors, one containing Cas9 controlled by a tet-responsive element and three different gRNAs against *BOLA3* behind their own U6 promoters, and one containing a next-generation reverse tetracycline transactivator (mrtTA) under the control of the CAG promoter, were introduced into the parental Ins-GFP human embryonic stem cell line. This dual-vector system enables constitutive expression of mrtTA and the *BOLA3*-targeted gRNAs. Subsequent administration of doxycycline enables mrtTA to bind the tet-responsive element, thereby inducing Cas9 expression and gene editing (González et al., 2014) (Fig. 4-4A,B).

$BOLA3^{KO}$ clusters were treated with doxycycline for seven days, immediately post-sorting and reaggregation (day 20), or fourteen days, beginning at the transition between pancreatic progenitor cells into immature, beta-like cells (day 12) (Fig. 4-5). Given that day 12 spheres are still undergoing maturation, it should be noted that introduction of doxycycline at this stage may result in biological changes to the differentiation process itself. However, we observed little difference in GFP expression between Day 20 cells that began doxycycline treatment at Day 12 and their untreated counterparts. Treatment of $BOLA3^{KO}$ clusters with doxycycline for one week resulted in diminished BOLA3 in Day 20 spheres and reduced DLAT and DLST in Day 27 eBCs (Fig. 4-6A,B). Treated and untreated $BOLA3^{KO}$ eBCs were morphologically similar both seven and fourteen days post-doxycycline; however, while GFP expression was equivalent between treated and untreated eBCs seven days post-doxycycline, treated

BOLA3^{KO} eBCs exhibited diminished GFP expression in comparison to their untreated counterparts fourteen days post-doxycycline, indicative of reduced insulin promoter activity (Fig. 4-6C,D).

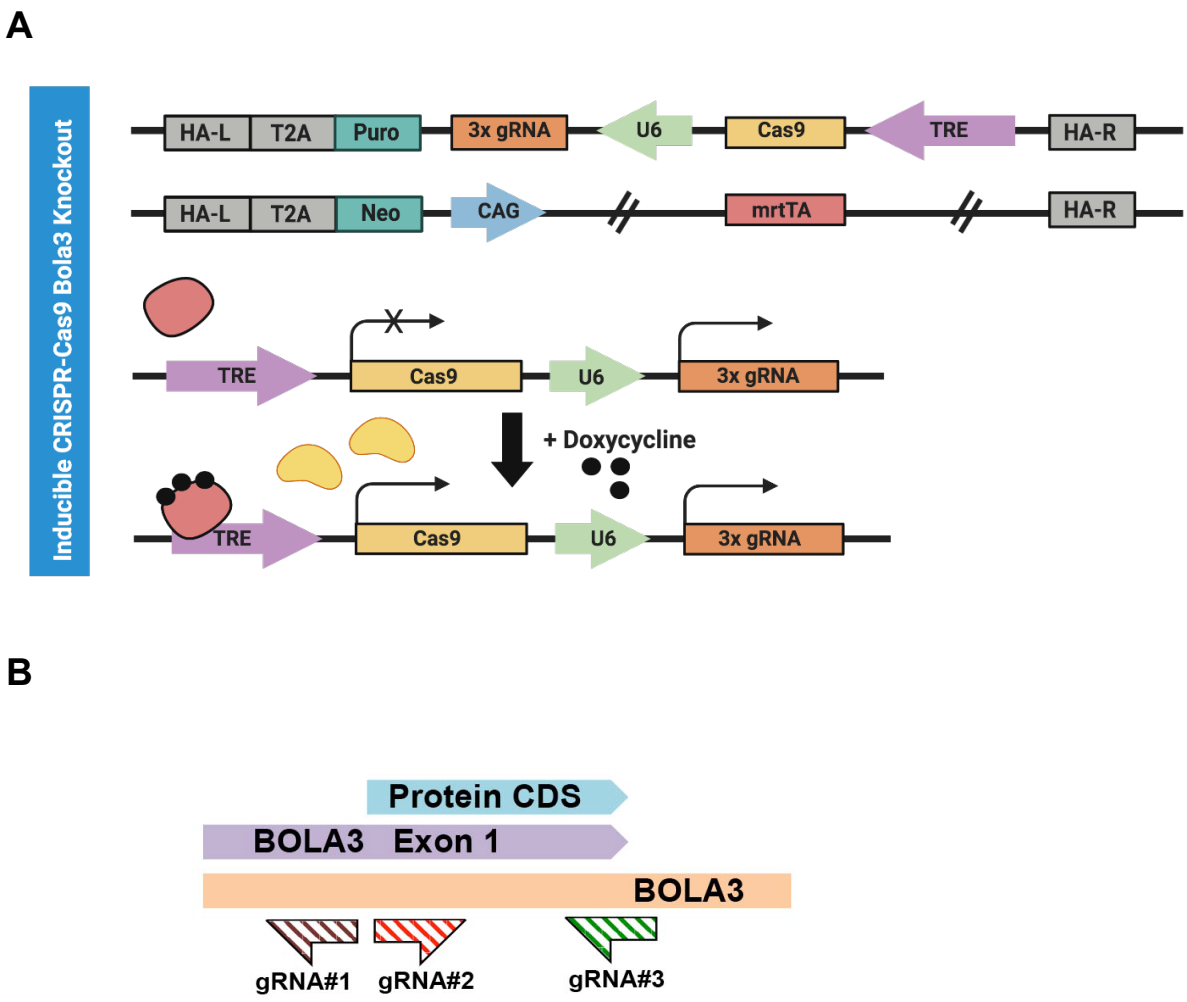

Figure 4-4. Generation of the CRISPR-based inducible *BOLA3* knockout hESC line. (A) Schematic representation of the dox-inducible *BOLA3*^{KO} CRISPR-Cas9 system. BOLA3^{KO} hESCs possess constructs including three ubiquitously expressed guide RNAs targeting *BOLA3*, an inducible Cas9, and ubiquitously-expressed mrtTA. Upon doxycycline treatment, mrtTA binds to the tet-responsive promoter, inducing expression of Cas9 and subsequent *BOLA3* gene editing. (B) Guide RNA binding sites within exon one of the human *BOLA3* gene.

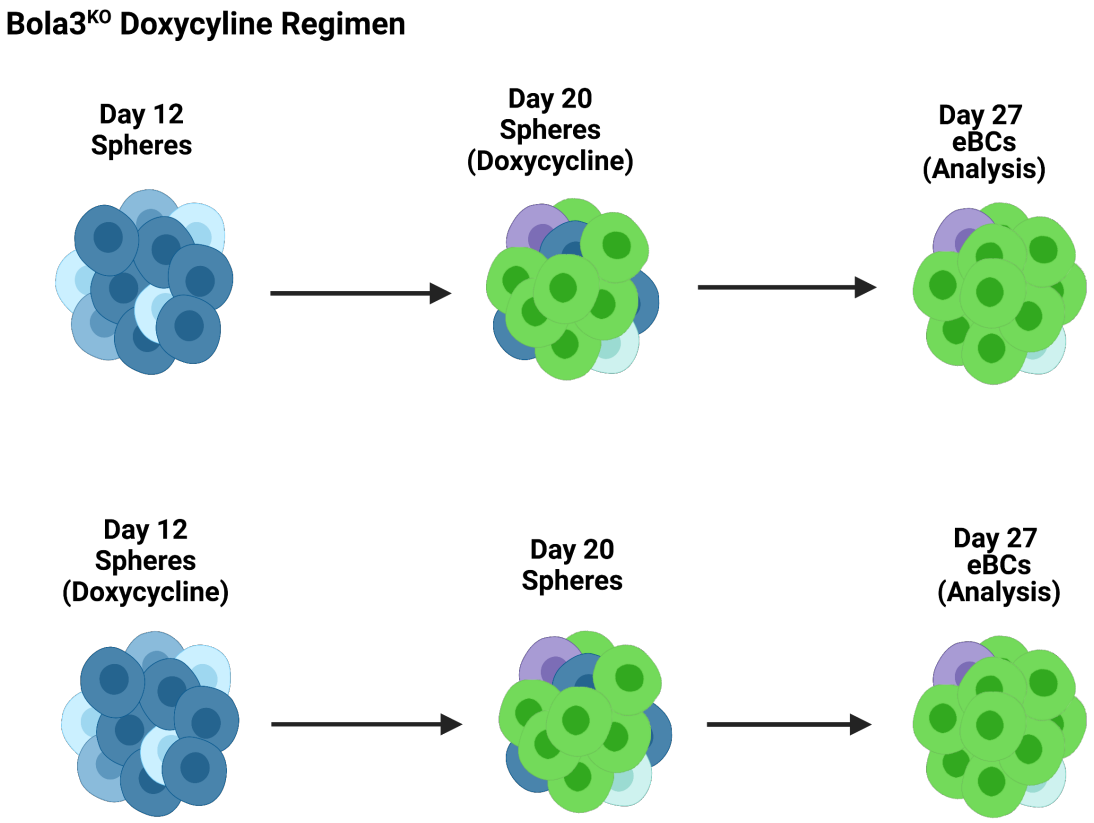

Figure 4-5. Doxycycline treatment regimen of BOLA3^{KO} clusters. Schematic representing each doxycycline treatment strategy utilized. Doxycyline treatment began at either beta cluster reaggregation (Day 20, seven total days of doxycycline treatment) or at the pancreatic progenitor stage of differentiation (Day 12, fourteen total days of doxycycline treatment). eBCs subjected to both regimens were analyzed at Day 27.

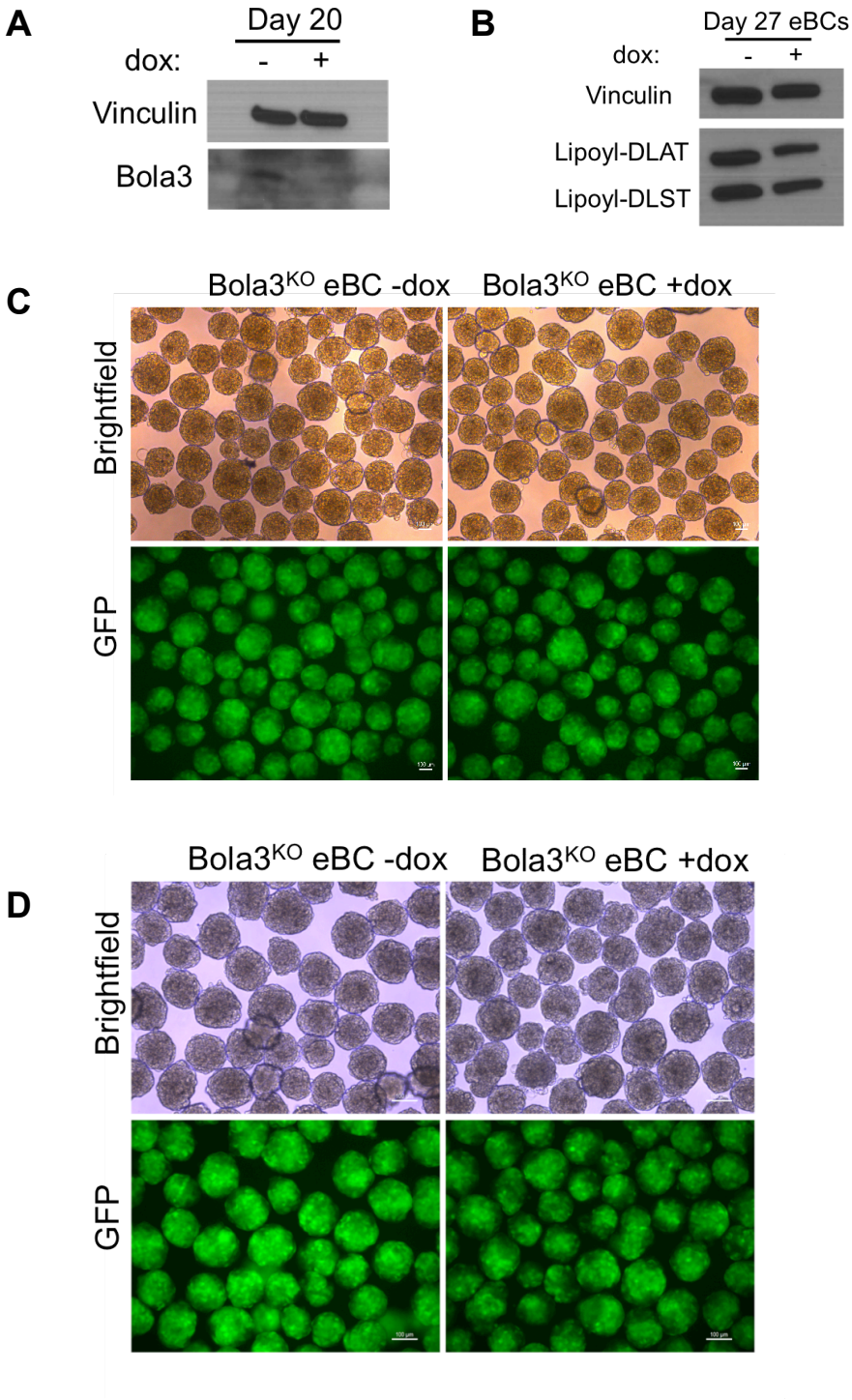

Figure 4-6. Validation of the *BOLA3*^{KO} line. (A,B) Western blot for BOLA3 in Day 20 beta-like clusters (A) and DLAT and DLST in Day 27 eBCs (B) seven days post-doxycycline. (C,D) Representative brightfield and GFP images of Day 27 eBCs seven days (C) or fourteen days (D) post-doxycycline.

Dynamic glucose-stimulated insulin secretion assays were used to perform functional assessments of BOLA3^{KO} eBCs. Following one week of doxycycline treatment, Day 27 BOLA3^{KO} eBCs began to exhibit diminished glucose-stimulated insulin secretion, as measured by both absolute c-peptide secreted and stimulation index over the course of the assay (Fig. 4-7A,B), though the functional variability between individual differentiations of BOLA3^{KO} eBCs precluded appropriate statistical analysis of elements of these data. Extension of the doxycycline treatment regimen to fourteen days, however, significantly worsened the secretory capacity of Day 27 BOLA3^{KO} eBCs (Fig. 4-7C,D). Rather than displaying a simple reduction in secretion compared to untreated eBCs, Day 27 BOLA3^{KO} eBCs treated with doxycycline for fourteen days appeared to lose the ability to secrete insulin upon glucose stimulation. Under both treatment regimens doxycyline treatment most heavily impacted first-phase insulin secretion, which we define as the secretory peak between minutes twenty-four and twenty-right (24'-28') over the course of the assay (Fig. 4-7E,F). This result suggests that loss of *Bola3* in Day 27 BOLA3^{KO} eBCs likely affects either the production or trafficking of insulin granules, or the secretion of insulin granules belonging to the readily releasable pool (RRP), which largely comprise the first-phase insulin response (Hou et al., 2009).

.

A

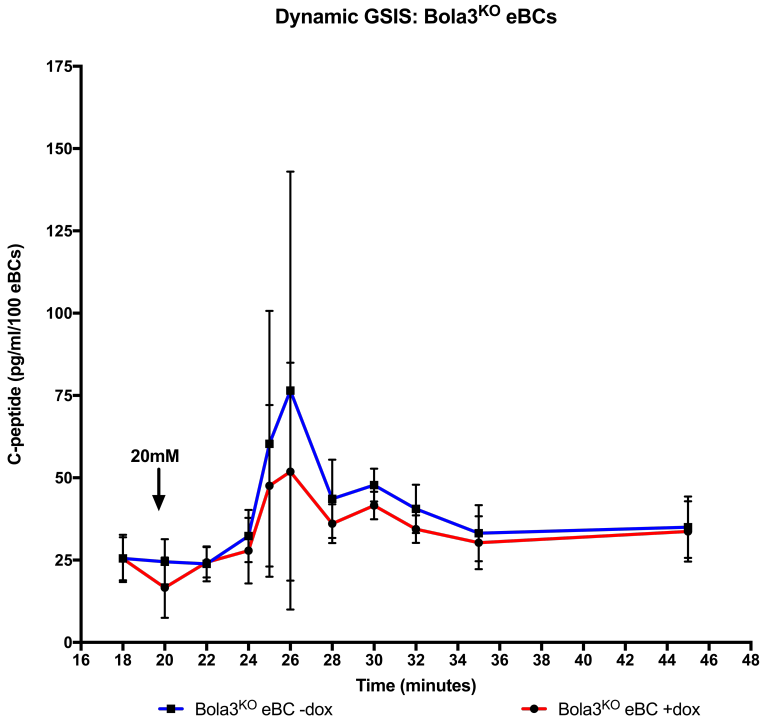

B

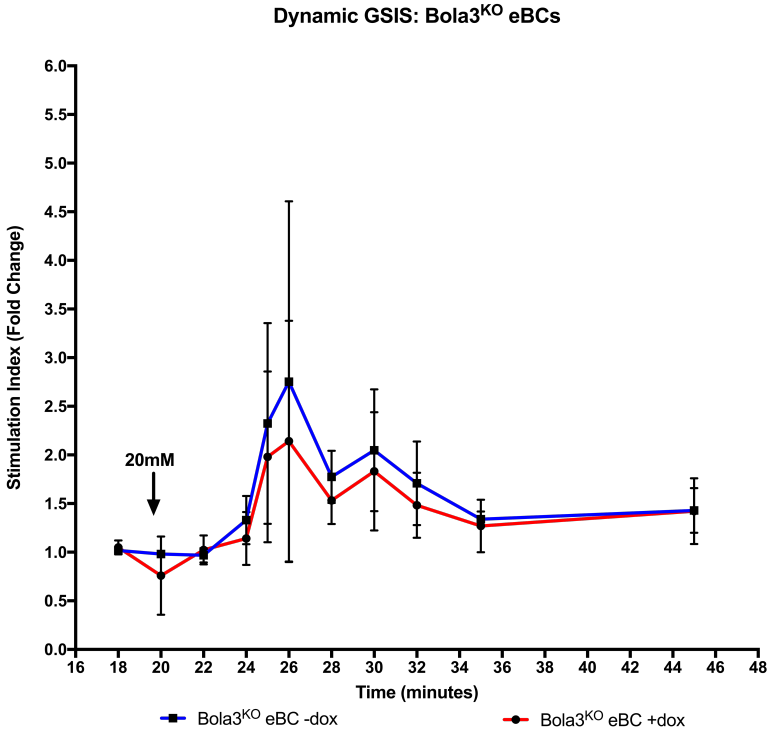

Figure 4-7. BOLA3 knockout in eBCs results in diminished insulin secretion. Reduction of BOLA3 led to decreased c-peptide and stimulation index both seven (A,C) and fourteen (B,D) days post-doxycycline. (E,F) Area under the curve representation of (C), (D) during first-phase insulin secretion (24' - 28').

C

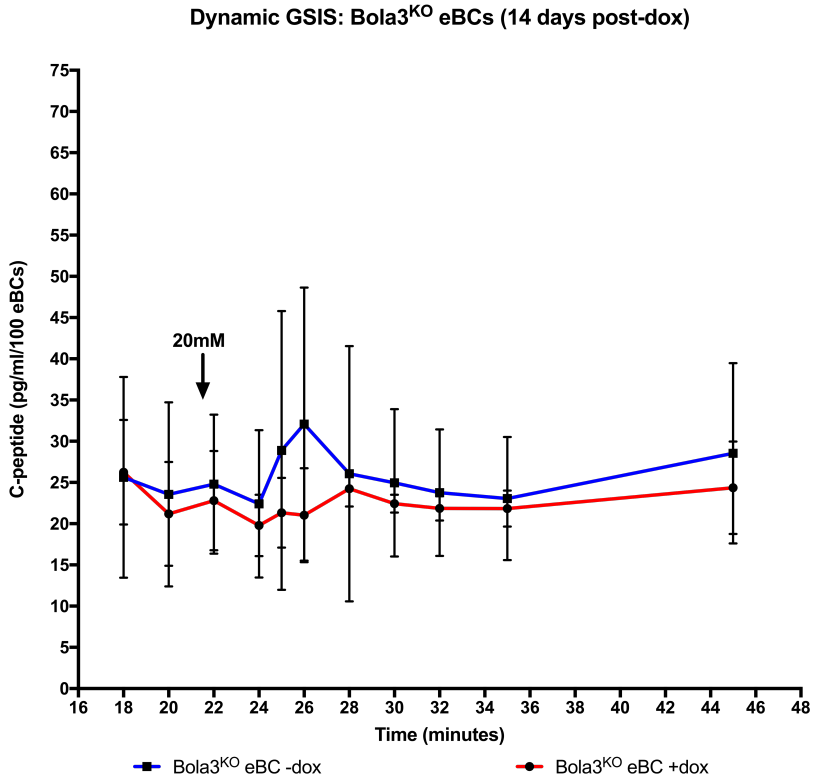

D

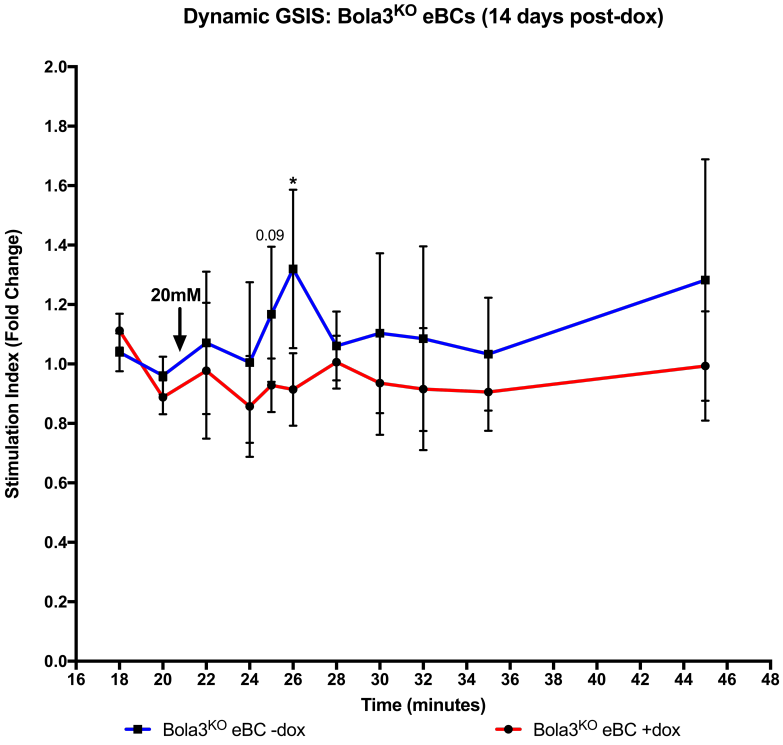

Figure 4-7. BOLA3 knockout in eBCs results in diminished insulin secretion (cont'd).

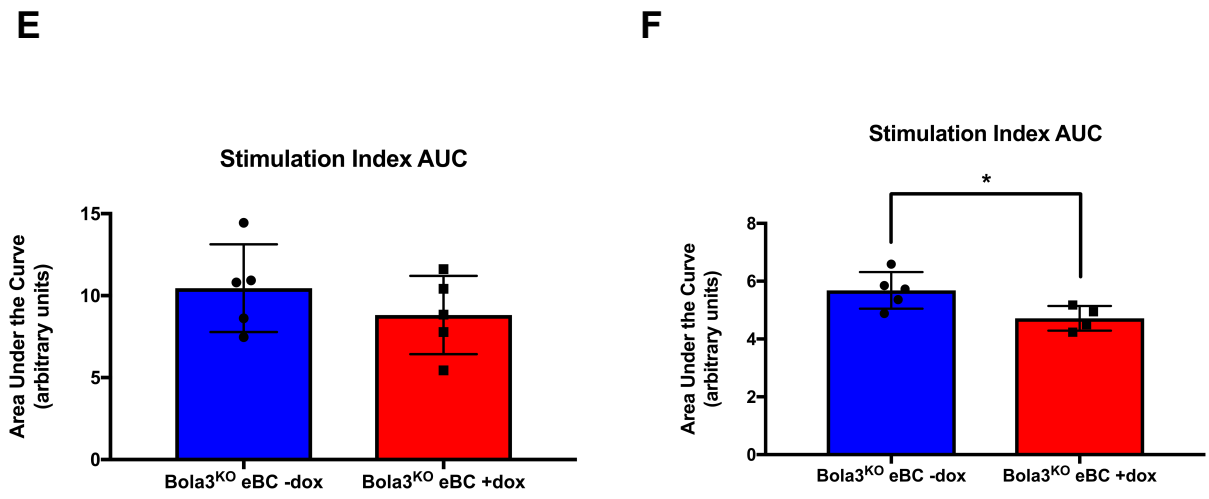

Figure 4-7. BOLA3 knockout in eBCs results in diminished insulin secretion (cont'd).

Inducible Bola3 overexpression in human stem cell-derived beta cells

To probe whether augmenting endogenous BOLA3 expression in hESC-derived beta cells could improve their metabolic and functional capacity we generated a doxycycline-inducible *Bola3* overexpression hESC line ($BOLA3^{OE}$). Using TALEN technology, as with the generation of the $BOLA3^{KO}$ hESC line, Ins-GFP hESCs were electroporated with an hAAVS1-targeted vector containing a Tet-On bidirectional inducible expression system. In this system, constitutive expression of the tet-on transactivator protein is driven by the CAG promoter; administration of doxycycline enables binding of the constitutively-expressed tet-on transactivator protein to a third generation tet-responsive promoter, thereby driving expression of the BOLA3 coding sequence (Fig. 4-8).

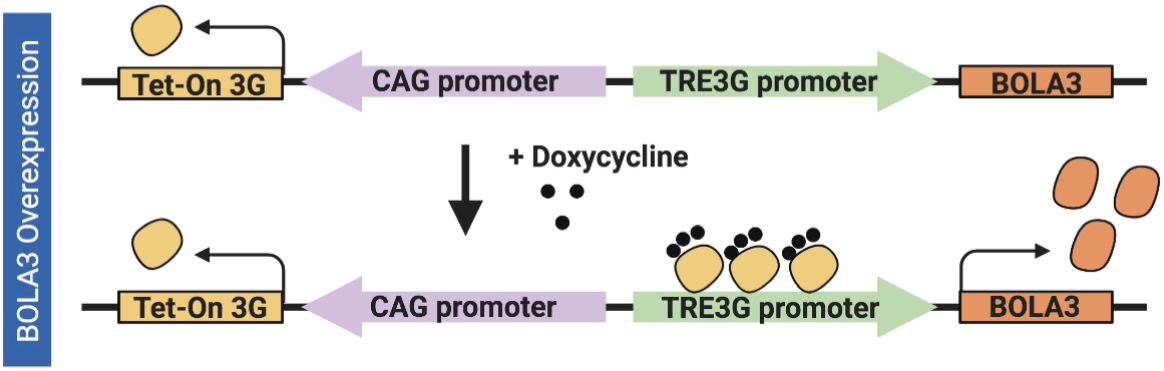

Figure 4-8. Generation of the BOLA3^{OE} overexpression hESC line. Schematic representation of the doxycycline-inducible BOLA3^{OE} hESC line. Upon doxycycline treatment, the ubiquitously expressed tet-on transactivator protein binds to the tet-responsive promoter, inducing *BOLA3* overexpression.

Following 48 hours of doxycycline treatment BOLA3^{OE} eBCs were analyzed at either seven (Day 27) or fourteen (Day 34) days following sorting and reaggregration (Fig. 4-9A). Treatment of Day 27 BOLA3^{OE} eBCs with doxycycline for 48 hours led to a significant increase in total BOLA3 protein with no apparent change in eBC morphology (Fig. 4-10A, C). Intriguingly, the increase in lipoylated DLAT and DLST appeared relatively moderate (Fig. 4-10B,C). These data speak to a similar notion as that derived from the *Bola3*^{KO} mouse model: namely, that observable phenotypes may occur in the presence of partial or subtle changes in BOLA3 target protein lipoylation. This may suggest that enhanced protein lipoylation is capable of serving as a particularly robust driver of downstream cellular processes; or, alternatively, that the functional consequences of BOLA3 loss or overexpression arise largely from its impact on mitochondrial respiratory chain complexes, rather than protein lipoylation.

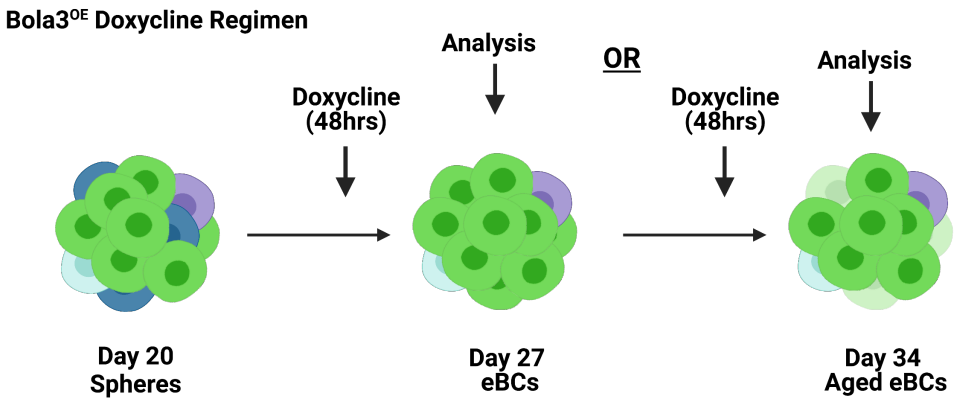

Figure 4-9. Treatment and analysis timeline of Bola3^{OE} eBCs. BOLA3^{OE} eBCs were treated with doxycyline at either Day 25 or Day 32 to facilitate analysis 48hrs post-doxycyline at Day 27 in mature eBCs or Day 34 in “aged” eBCs.

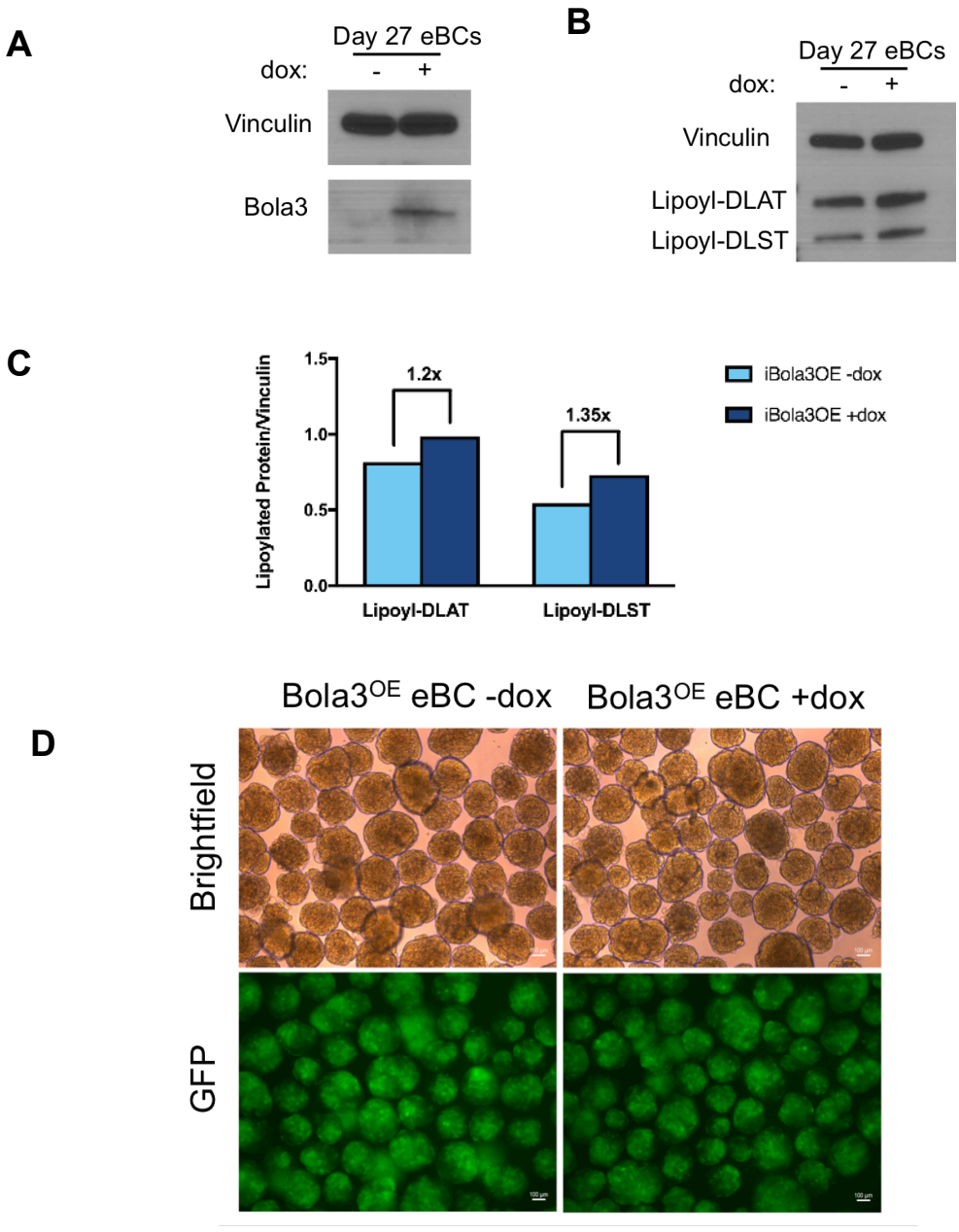

Figure 4-10. Validation of the *BOLA3*^{OE} line. (A) Western blot for BOLA3 in Day 27 BOLA3^{OE} eBCs following 48hrs of doxycyline treatment. (B) Western blot for lipoylation of downstream BOLA3 targets DLAT and DLST in Day 27 BOLA3^{OE} eBCs 48hrs post-doxycycline. (C) Representative brightfield and GFP images of BOLA3^{OE} eBCs 48hrs post-doxycycline.

We subsequently determined that induction of supraphysiological BOLA3 through doxycyline treatment enhanced glucose-stimulated insulin secretion in Day 27 BOLA3^{OE} eBCs, as measured both by the absolute amount of c-peptide secreted upon exposure to high glucose and the stimulation index of BOLA3^{OE} eBCs (Fig. 4-11A,B). This improvement was evident at both discrete secretory timepoints and over the sum total of the first-phase glucose response (Fig. 4-11C). Treated and untreated Day 27 BOLA3^{OE} eBCs secrete equivalent c-peptide at low glucose, indicating that the functional improvement resulting from BOLA3 overexpression under these conditions is tightly controlled and linked to the physiological glucose response. Similarly, we observed no difference in total insulin content between treated and untreated Day 27 BOLA3^{OE} eBCs (Fig. 4-11D). Given that extended culturing of Ins-GFP eBCs *in vitro* results in mild functional degradation, we additionally sought to assess the impact of BOLA3 overexpression on "aged" Day 34 BOLA3^{OE} eBCs. Treatment with doxycycline for 48 hours restored the function of Day 34 BOLA3^{OE} eBCs, increasing both the absolute amount of c-peptide secreted upon exposure to high glucose and stimulation index (Fig. 4-12A,B). Unlike treated Day 27 BOLA3^{OE} eBCs, however, treated Day 34 BOLA3^{OE} eBCs secreted more insulin at under low glucose conditions than untreated Day 34 BOLA3^{OE} eBCs.

A

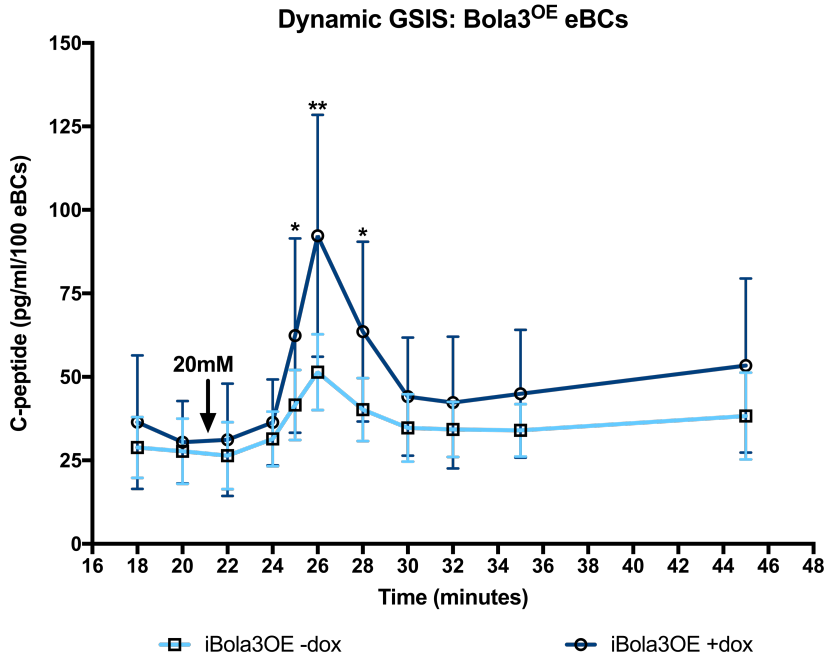

B

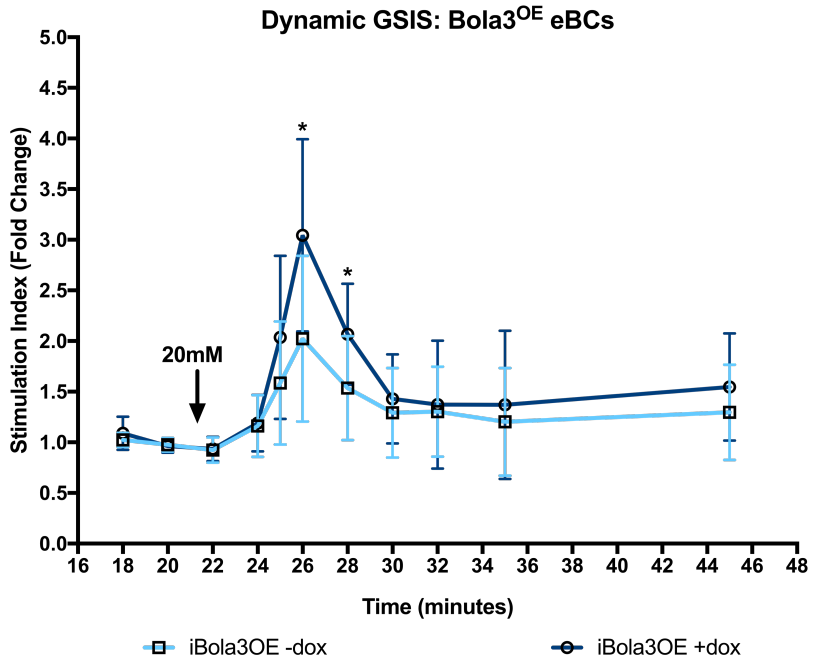

Figure 4-11. Overexpression of BOLA3 in Day 27 BOLA3^{OE} eBCs improves glucose-stimulated insulin secretion. (A,B) Overexpression of BOLA3 in doxycycline-treated Day 27 eBCs led to increased c-peptide (A) and stimulation index (B) following glucose stimulation. (C) Area under the curve representation of (B) during first-phase insulin secretion (24' - 28'). (D) Total insulin content of untreated and treated BOLA3^{OE} eBCs.

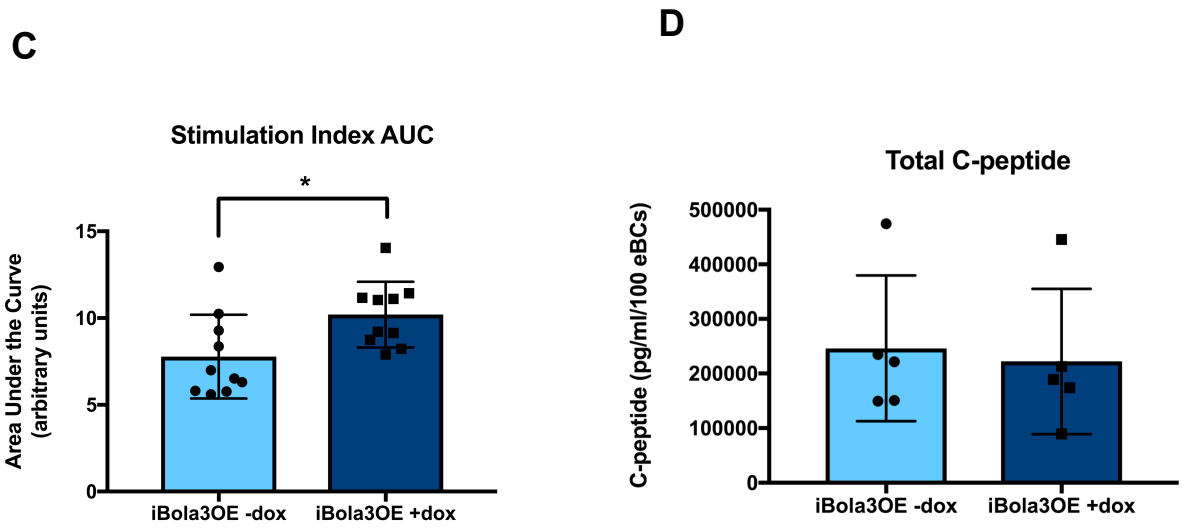

Figure 4-11. Overexpression of BOLA3 in Day 27 BOLA3^{OE} eBCs improves glucose-stimulated insulin secretion (cont'd).

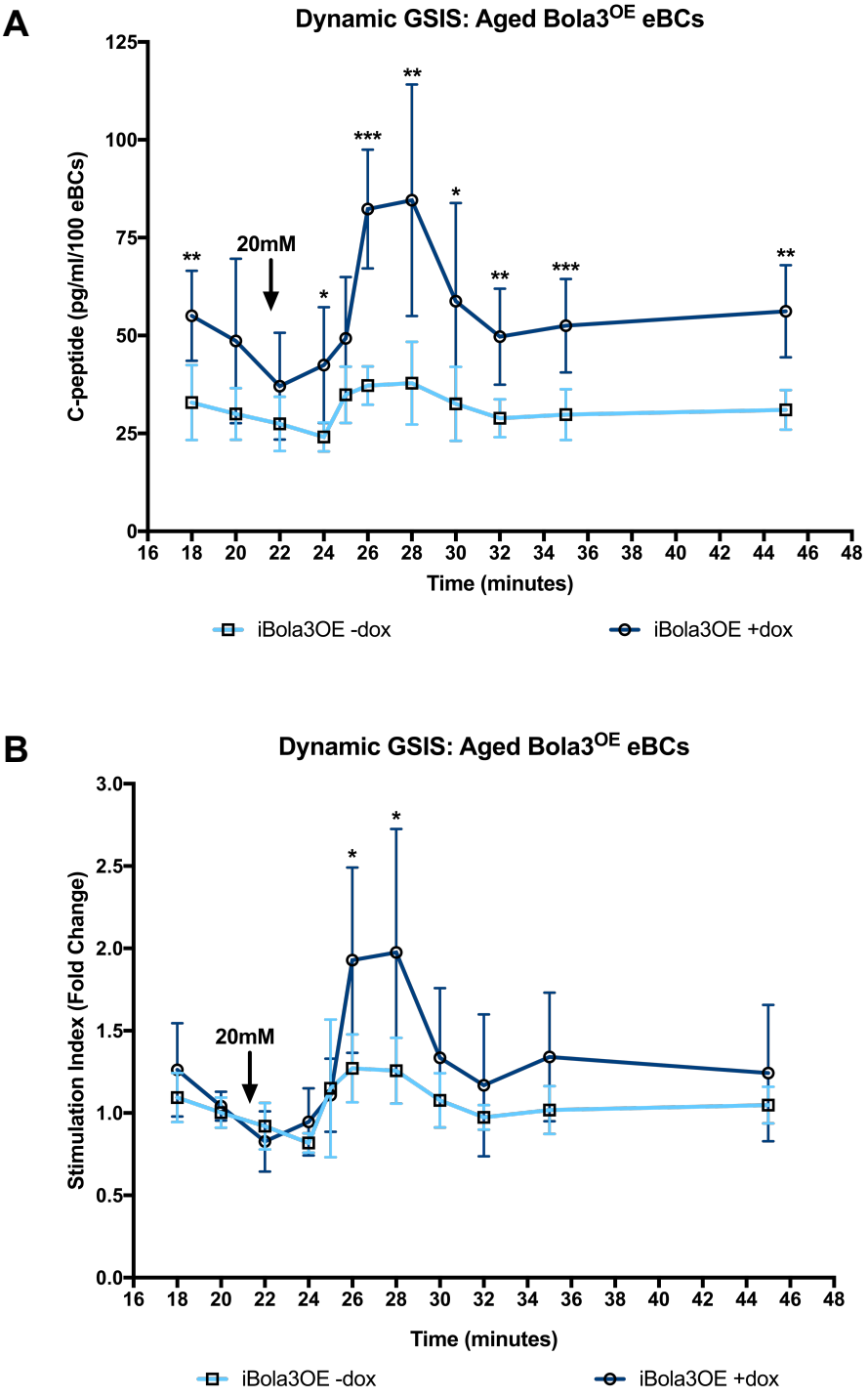

Figure 4-12. Overexpression of BOLA3 in Day 34 BOLA3^{OE} eBCs improves glucose-stimulated insulin secretion. (A,B) Overexpression of BOLA3 in doxycycline-treated Day 34 eBCs led to increased c-peptide (A) and stimulation index (B) following glucose stimulation.

Discussion:

Clinical data from *Bola3*-deficient MMDS patients and RNA sequencing data of both hESC-derived beta cells and human islets suggested that *Bola3* likely plays a role in the human beta cell. Upon transitioning to an *in vitro* hESC-derived beta cell system, we determined that *Bola3* loss diminished glucose-stimulated insulin secretion. The severity of these impairments was positively correlated with the length of doxycycline treatment, which may be linked to an increased window for either CRISPR-Cas9 activity or degradation of remaining BOLA3 protein. This would appear to recapitulate of our observations in *Bola3*^{KO} mice, which demonstrate a gradual, rather than immediate, decline in glucose tolerance. However, it should be noted that establishing a fourteen day treatment regimen requires that doxycycline be introduced to *Bola3* clusters at the beginning of terminal beta cell specification (Day 12), as opposed to the immature, beta-like stage (Day 20). It will therefore require further investigation to determine the degree to which the particular stage at which doxycycline is introduced, rather than simply the length of the doxycycline treatment itself, impacts the effect of *Bola3* knockout on BOLA3^{KO} eBCs.

Metabolic maturation has been shown to drive functional maturation in the beta cell (Yoshihara et al., 2016; Nair et al., 2019). For that reason, identifying novel regulators of beta cell metabolism, particularly those linked to mitochondrial function and dysfunction, may facilitate both the improvement of *in vitro* beta cell differentiation and the development of novel therapeutic strategies for type 2 diabetes. Our data demonstrate that supraphysiological *Bola3* expression in hESC-derived beta cells improves glucose-stimulated insulin secretion *in vitro*; these improvements are apparent in both normal, functional beta cells and beta cells that have experienced functional

degradation. This is critical, given that the prevalence of beta cell dysfunction in type 2 diabetes requires that potential therapeutic interventions be capable of rescuing function, rather than simply improving existing function.

As a post-translational modifier within the mitochondria, *BOLA3* represents a particularly intriguing therapeutic target. The functional improvements observed upon its overexpression suggest that beta cell metabolism and function may be improved through precise augmentation of specific mitochondrial and metabolic factors, rather than the wholesale shifts in cellular transcriptional profiles resulting from altered expression of transcription factors that broadly regulate metabolism. While this study is focused on BOLA3, this concept may be applicable to other regulators of mitochondrial function, including the downstream BOLA3 targets PDH, aKGDH, and the mitochondrial respiratory chain complexes. Increased expression and activity of these factors may result in the overproduction of reactive oxygen species within the mitochondria, a possibility that requires careful assessment. Still, the promise of BOLA3 and its ilk as therapeutic strategies for type 2 diabetes patients warrants continued investigation.

CHAPTER 5.

Materials & Methods

Mouse Studies

Pdx1^{CreER} and *Bola3* floxed (Bola3$^{tm1a(EUCOMM)Wtsi}$) mice were obtained from Dr. Doug Melton and Dr. Shingo Kajimura, respectively. At eight weeks of age Bola3$^{flox/wt}$, Bola3$^{flox/flox}$, Pdx1Cre^{ER};Bola3$^{flox/+}$, and Pdx1Cre^{ER};Bola3$^{flox/flox}$ mice were injected with 100ul of 10mg/ml tamoxifen dissolved in corn oil daily for five days. IPGTT analyses were carried out at two, four, six, and eight months following administration of tamoxifen. Mice were weighed after a 16-18hr fast. Fasted blood glucose levels were measured using the Contour Glucometer and mice were injected intraperitoneally with a 1M glucose solution at 10 µl per gram of body weight. Blood glucose was measured at 15min, 30min, and every 30min thereafter for 150min post-injection. ITT analyses were carried out on six and eight month-old male Bola3$^{flox/wt}$, Bola3$^{flox/flox}$, Pdx1Cre^{ER};Bola3$^{+/-}$, and Pdx1Cre^{ER};Bola3$^{-/-}$ mice according to the IPGTT protocol described above, with injections of 1U insulin per kilogram of body weight. Tail-vein blood was taken for *in vivo* glucose-stimulated insulin measurements prior to glucose injection and 30min post-injection. Samples were spun down to collect serum and stored at −80°C with protease inhibitors (Roche). Insulin concentration was calculated using the Rodent Insulin ELISA kit (ALPCO). All animals were maintained in the barrier facility according to protocols approved by the Committee on Animal Research at the University of California, San Francisco.

Immunofluorescent Staining

Murine pancreata were fixed in Z-Fix (Anatech) for 12–16 h at 4°C and processed for paraffin embedding. Pancreatic sections were de-paraffinized, rehydrated, permeabilized with PBST (0.2% Tween-20 in 1X PBS), and subjected to antigen retrieval by boiling in a water bath in 1X Antigen Retrieval Citra Plus Solution (BioGenex) for 10min at moderate power, followed by 2min at low power. After cooling to room temperature, slides were washed three times in PBS for 10min each and incubated in blocking buffer (10% FBS in PBST) for 1hr, followed by incubation with primary antibodies in blocking buffer overnight at 4°C. Slides were washed three times with PBST for 10min each, followed by incubation for 2hr at room temperature with secondary antibodies in blocking buffer. Slides were washed three times in PBST for 10min each and mounted using ProLong Diamond Antifade Mountant with DAPI (Invitrogen). Day 20 hESC-derived beta-like spheres and eBCs were fixed with 4% PFA for 15min at room temperature, washed with PBS, and stored at 4°C. Spheres and eBCs were later embedded in 2% agar, followed by dehydration, paraffin embedding and sectioning. Sections were then stained according to the above protocol.

RNA Isolation and Quantitative PCR

RNA isolation was carried out using the RNeasy kit (Qiagen) as per manufacturer's instructions. cDNA preparation was carried out using the SuperScript III First Strand synthesis kit (ThermoFisher Scientific), and quantitative PCR (qPCR) were performed using FastStart SYBR Green Master Mix (Roche) as per manufacturer's instructions. Target gene expression was normalized to either murine Cyclophilin A or human TBP. Fast SyBr green was used for all qPCR reactions.

Protein Isolation and Western Blotting

Isolated mouse islets or hESC-derived clusters were lysed in 10X PhosSTOP (Roche), 25X protease inhibitor (Roche), and 100X PMSF in RIPA buffer (Pierce). Protein concentration was measured using the Pierce BCA Protein Assay Kit (Thermo Scientific) as per manufacturer's instructions. Cell lysates were resolved on 10% or 4-20% acrylamide gradient SDS–PAGE Mini-Protean TGX gels (Bio-Rad). Samples were transferred to PVDF membranes (Bio-Rad), blocked for 1hr at room temperature in TBST (0.05% Tween-20 in 1X TBS) with 5% milk, and incubated overnight at 4°C with primary antibodies in TBST with 1% milk. Membranes were washed three times for 20min each with TBST and incubated for 2hr at room temperature with secondary antibodies in TBST with 1% milk. Membranes with washed three times for 20min each, incubated for 5min with SuperSignal™ West Pico Plus Chemi-luminescent Substrate (Thermo Scientific), and developed.

Seahorse Metabolic Analysis

Real-time mitochondrial respiration and oxygen consumption rate (OCR) was measured using an XFe24 extracellular flux analyzer (Seahorse Bioscience). Mouse islets were isolated at six months post-tamoxifen and rinsed with sodium bicarbonate-free, pH adjusted (7.4) XF base media supplemented with 3mM glucose. 50 islets were placed in each well of an islet capture plate, with three replicates per animal. After insertion of a mesh into each well to prevent movement of clusters during the assay, the plate was incubated in a non-CO_2 incubator at 37°C for one hour. Basal oxygen consumption rates were measured at 3mM glucose. Glucose (3mM or 20mM),

oligomycin (5uM), carbonyl cyanide-4-(trifluoromethoxy) phenylhydrazone (FCCP, 1uM), and rotenone and antimycin A (5uM) were then injected sequentially over the course of the assay. OCR was measured at 37°C in real time throughout the assay period. OCR was normalized to average baseline measurement and expressed as percent change during the course of the experiment. Insulin and DNA content of each well were also determined by STELLUX Chemi Human C-peptide ELISA kit (Alpco) and Quant-iT PicoGreen dsDNA Assay Kit, respectively.

Static Glucose-Stimulated Insulin Secretion Assay

Islets from adult mice were isolated by the Islet Production Facility Core at the Diabetes Center at University of California at San Francisco. Twenty-five islets per 5ml tube underwent a one hour-long equilibration period in Krebs-Ringer buffer (KRB) with 2.8mM glucose. Islets were provided with fresh KRB with 2.8mM glucose and incubated for one hour at 37°C. Islets were then incubated for one hour with either fresh KRB with 2.8mM glucose, KRB with 2.8mM glucose and recombinant BOLA3 protein (rBOLA3) at 50ug/ml, KRB with 16.7mM glucose, or KRB with 16.7mM glucose and rBOLA3 at 50ug/ml. Following pre-incubation, samples were at the end of each hour-long incubation to quantify insulin secretion. Insulin levels were measured using the STELLUX Rodent Insulin Chemiluminescence ELISA kit (Alpco). Dosage response to rBOLA3 was measured as described above, incubating islets in either KRB with 16.7mM glucose or KRB with 16.7mM glucose and 25mg/ml, 50mg/ml, or 100mg/ml rBOLA3. Human islets were isolated by the Islet Production Facility Core at the Diabetes Center at University of California at San Francisco and subjected to the procedure described above, utilizing KRB with 3mM glucose, KRB with 20mM glucose,

or KRB with 20mM glucose and 50mg/ml rBOLA3. C-peptide levels were measured using the STELLUX Chemi Human C-peptide ELISA kit (Alpco).

Cell Culture and Fluorescence-Activated Cell Sorting

Mel1 INSGFP/W human embryonic stem cells were maintained and propagated on mouse embryonic fibroblasts (MEFs) in hESC media. Cells were passaged by enzymatic dissociation using TrypLE (Gibco). To initiate differentiation, confluent hESC cultures were dissociated into single-cell suspensions using TrypLE and seeded at $5.5x10^6$ cells/well in six-well suspension plates, each with 5.5ml hESC media supplemented with 10 ng/ml activin A (R&D Systems) and 10 ng/ml heregulinB (Peprotech). Suspension plates were incubated at 37°C and 5% CO_2 on an orbital shaker at 100 rpm to induce 3D sphere formation. After 24 hours, spheres were collected in 50 ml falcon tubes, allowed to settle by gravity, washed once with RPMI, and resuspended in day 1 media. Following resuspension in day 1 media, spheres were distributed into fresh six-well suspension plates with 5.5ml of media/well. Media was changed every day thereafter. Until day 3 spheres were fed by removing 5ml of the media and replenishing with 5.5 ml of media. From days 4 through 20, 4.5ml of media was removed from each well and replaced with 5ml of fresh media. Media compositions are as follows:

Day 1: RPMI (Gibco) containing 0.2% FBS, 1:5,000 ITS (Gibco), 100ng/ml activin A, and 50ng/ml WNT3a (R&D Systems).

Day 2: RPMI containing 0.2% FBS, 1:2,000 ITS, and 100ng/ml activin A.

Day 3: RPMI containing 0.2% FBS, 1:1,000 ITS, 2.5μM TGFbi IV (CalBioChem), and 25ng/ml KGF (R&D Systems).

Day 4–5: RPMI containing 0.2% FBS, 1:1,000 ITS, and 25ng/ml KGF.

Day 6–7: DMEM (Gibco) with 25mM glucose containing 1:100 B27 (Gibco) and 3nM TTNPB (Sigma). Day 8: DMEM with 25mM glucose containing 1:100 B27, 3nM TTNPB and 50ng/ml EGF (R&D Systems).

Day 9–11: DMEM with 25mM glucose containing 1:100 B27, 50ng/ml EGF, and 50ng/ml KGF.

Day 12–20: DMEM with 25mM glucose containing 1:100 B27, 1:100 Glutamax (Gibco), 1:100 NEAA (Gibco), 10μm ALKi II (Axxora), 500nM LDN-193189 (Stemgent), 1μm Xxi (Millipore), 1μM T3 (Sigma-Aldrich), 0.5mM vitamin C, 1mM N-acetyl cysteine (Sigma-Aldrich),10μM zinc sulfate (Sigma-Aldrich) and 10 μg/ml of heparin sulfate.

Day 20: spheres were collected and dissociated into single cell suspensions using Accumax, for FACS. Live GFP^{high} cells were sorted on FACSAria II machines at low flow rates and reaggregated in Aggrewell-400 (StemCell Technologies) plates at $1.2x10^6$ cells/well in CMRL containing 1:100 B27, 1:100 Glutamax (Gibco), 1:100 NEAA (Gibco), 10μm ALKi II (Axxora), 0.5mM vitamin C, 1μM T3 (Sigma-Aldrich), 1mM N-acetyl Cysteine (Sigma-Aldrich), 10μM zinc sulfate (Sigma-Aldrich) and 10μg/ml of heparin sulfate.

Day 23: reaggregated enhanced beta clusters (eBCs) were transferred from Aggrewells into six-well suspension plates and incubated on orbital shakers at 37°C, 5% CO_2, and 100 rpm. eBCs were further cultured for one to two weeks. Media was changed every third day following reaggregation. A step-by-step protocol describing the maintenance of

undifferentiated hESCs, differentiation of hESCs to beta cells, and FACS is published at Nair et al., 2019.

Generation of Bola3^{OE} and Bola3^{KO} cell lines

To generate the Bola3^{OE} cell line, human Bola3 cDNA (Genscript #OHu17882) was subcloned into the AAVS1-TRE3G-EGFP plasmid (Addgene #52343) to generate a doxycycline-inducible AAVS1-TRE3G-Bola3 plasmid. Mel1-INS$^{GFP/WT}$ human embryonic stem cells were dissociated into single cells with TrypLE Select and quenched. Eight million cells were resuspended in 500ul hESC maintenance media (hESCa + FGF2) then combined in a 0.4cm gap cuvette with 300ul PBS$^{+/+}$, 20ug AAVS1-TRE3G-Bola3 plasmid, and 5ug each of AAVS1-TALEN-R and AAVS1-TALEN-L plasmids. Cell resuspension mix was electroporated using the Gene Pulser Xcell (Biorad) and replated on DR4 iMEFs (Thermo Scientific) with hESC maintenance media and rock inhibitor. Single colonies were picked following one week of selection with 0.5ug/ml puromycin and propagated for freezing and genomic DNA, RNA, and protein extraction to confirm insertion and induction capacity of the AAVS1-TRE3G-Bola3 construct. To generate the Bola3^{KO} cell line, guide RNAs targeting exon 1 of the human BOLA3 sequence were designed using the online Benchling CRISPR Guide RNA design tool (https://www.benchling.com/crispr/). Guide RNA oligos were ordered from Integrated DNA Technologies (IDT) and annealed *in vitro* using 10uM top oligo, 10uM bottom oligo, and 5X Annealing Buffer (50mM Tris-HCl, 0.5M NaCl, 5mM EDTA). Three guide RNA sequences were sequentially subcloned into a modified pCR Blunt II TOPO plasmid (Invitrogen) containing U6 promoter and guide RNA tracr elements (gRNA donor plasmid). This 3x U6-sgRNA-tracr cassette was then subcloned into a Cas9-Puro

gRNA receiver plasmid (Addgene 58409), which was introduced concurrently with the Neo-M2rtTA plasmid (Addgene 60843a) into Mel1-INS$^{GFP/WT}$ human embryonic stem cells as described above.

Dynamic Glucose-Stimulated Insulin Secretion Assay

A perifusion system from Biorep technologies was used for dynamic secretion assays. 100 eBCs were suspended between layers of polyacrylamide beads (Biorad) in plastic chambers fitted with fiberglass filters and maintained at 37°C in a temperature- and CO_2-controlled chamber. The eBCs were perfused at 100 µl/min with Krebs-Ringer buffer (KRB) using a peristaltic pump. After an initial 60-90min long preincubation period in KRB with 2.8mM glucose, clusters were perfused with KRB with 2.8mM glucose for 20min, KRB with 20mM glucose for 30min, KRB with 2.8mM glucose for 20min, and KRB with 20mM glucose and 30mM KCL for 5min. Flowthrough was collected over the course of the experiment. After the experiment, clusters were recovered from the chambers and total insulin was collected using acid-ethanol extraction. C-peptide levels were measured using the STELLUX Chemi Human C-peptide ELISA kit (Alpco).

Works Cited

Alberts B, Johnson A, Lewis J, et al. Molecular Biology of the Cell. 4th edition. New York: Garland Science; 2002. Available from: https://www.ncbi.nlm.nih.gov/books/NBK21054/

Ahting, U., Mayr, J. A., Vanlander, A. V., Hardy, S. A., Santra, S., Makowski, C., Alston, C. L., Zimmermann, F. A., Abela, L., Plecko, B., Rohrbach, M., Spranger, S., Seneca, S., Rolinski, B., Hagendorff, A., Hempel, M., Sperl, W., Meitinger, T., Smet, J., … Haack, T. B. (2015). Clinical, biochemical, and genetic spectrum of seven new patients with NFU1 deficiency. *Frontiers in Genetics*, *6*(MAR). https://doi.org/10.3389/fgene.2015.00123

Backe, M. B., Moen, I. W., Ellervik, C., Hansen, J. B., & Mandrup-Poulsen, T. (2016). Iron Regulation of Pancreatic Beta-Cell Functions and Oxidative Stress. In *Annual Review of Nutrition* (Vol. 36, pp. 241–273). Annual Reviews Inc. https://doi.org/10.1146/annurev-nutr-071715-050939

Bai, N., Ma, J., Alimujiang, M., Xu, J., Hu, F., Xu, Y., Leng, Q., Chen, S., Li, X., Han, J., Jia, W., Bao, Y., & Yang, Y. (2021). Bola3 Regulates Beige Adipocyte Thermogenesis via Maintaining Mitochondrial Homeostasis and Lipolysis. *Frontiers in Endocrinology*, *11*. https://doi.org/10.3389/fendo.2020.592154

Baker, P. R., Friederich, M. W., Swanson, M. A., Shaikh, T., Bhattacharya, K., Scharer, G. H., Aicher, J., Creadon-Swindell, G., Geiger, E., Maclean, K. N., Lee, W. T., Deshpande, C., Freckmann, M. L., Shih, L. Y., Wasserstein, M., Rasmussen, M. B., Lund, A. M., Procopis, P., Cameron, J. M., … Van Hove, J. L. K. (2014). Variant non ketotic hyperglycinemia is caused by mutations in LIAS, BOLA3 and the novel gene GLRX5. *Brain*, *137*(2), 366–379. https://doi.org/10.1093/brain/awt328

Banci, L., Camponeschi, F., Ciofi-Baffoni, S., & Muzzioli, R. (2015). Elucidating the Molecular Function of Human BOLA2 in GRX3-Dependent Anamorsin Maturation Pathway. *Journal of the American Chemical Society*, *137*(51), 16133–16143. https://doi.org/10.1021/jacs.5b10592

Besseiche, A., Riveline, J. P., Delavallée, L., Foufelle, F., Gautier, J. F., & Blondeau, B. (2018). Oxidative and energetic stresses mediate beta-cell dysfunction induced by PGC-1α. *Diabetes and Metabolism*, *44*(1), 45–54. https://doi.org/10.1016/j.diabet.2017.01.007

Blum, B., Hrvatin, S., Schuetz, C., Bonal, C., Rezania, A., & Melton, D. A. (2012). Functional beta-cell maturation is marked by an increased glucose threshold and by expression of urocortin 3. *Nature Biotechnology*, *30*(3), 261–264. https://doi.org/10.1038/nbt.2141

Burr, S. P., Costa, A. S. H., Grice, G. L., Timms, R. T., Lobb, I. T., Freisinger, P., Dodd, R. B., Dougan, G., Lehner, P. J., Frezza, C., & Nathan, J. A. (2016). Mitochondrial Protein Lipoylation and the 2-Oxoglutarate Dehydrogenase Complex Controls HIF1α Stability in Aerobic Conditions. *Cell Metabolism*, *24*(5), 740–752. https://doi.org/10.1016/j.cmet.2016.09.015

Cameron, J. M., Janer, A., Levandovskiy, V., MacKay, N., Rouault, T. A., Tong, W. H., Ogilvie, I., Shoubridge, E. A., & Robinson, B. H. (2011). Mutations in iron-sulfur cluster scaffold genes NFU1 and BOLA3 cause a fatal deficiency of multiple respiratory chain and 2-oxoacid dehydrogenase enzymes. *American Journal of Human Genetics*, *89*(4), 486–495. https://doi.org/10.1016/j.ajhg.2011.08.011

Cantley, J., Selman, C., Shukla, D., Abramov, A. Y., Forstreuter, F., Esteban, M. A., Claret, M., Lingard, S. J., Clements, M., Harten, S. K., Asare-Anane, H., Batterham,

R. L., Herrera, P. L., Persaud, S. J., Duchen, M. R., Maxwell, P. H., & Withers, D. J. (2009). Deletion of the von Hippel-Lindau gene in pancreatic β cells impairs glucose homeostasis in mice. *Journal of Clinical Investigation*, *119*(1), 125–135. https://doi.org/10.1172/JCI26934

CDC. (2020). *National Diabetes Statistics Report 2020. Estimates of diabetes and its burden in the United States.*

Cerf, M. E. (2013). Beta cell dysfunction and insulin resistance. In *Frontiers in Endocrinology* (Vol. 4, Issue MAR). https://doi.org/10.3389/fendo.2013.00037

Clark, E., Johnson, J., Dong, Y. N., Mercado-Ayon, E., Warren, N., Zhai, M., McMillan, E., Salovin, A., Lin, H., & Lynch, D. R. (2018). Role of frataxin protein deficiency and metabolic dysfunction in Friedreich ataxia, an autosomal recessive mitochondrial disease. *Neuronal Signaling*, *2*(4). https://doi.org/10.1042/ns20180060

Cnop, M., Mulder, H., & Igoillo-Esteve, M. (2013). Diabetes in Friedreich ataxia. In *Journal of Neurochemistry* (Vol. 126, Issue SUPPL.1, pp. 94–102). https://doi.org/10.1111/jnc.12216

Cohrs, C. M., Panzer, J. K., Drotar, D. M., Enos, S. J., Kipke, N., Chen, C., Bozsak, R., Schöniger, E., Ehehalt, F., Distler, M., Brennand, A., Bornstein, S. R., Weitz, J., Solimena, M., & Speier, S. (2020). Dysfunction of Persisting β Cells Is a Key Feature of Early Type 2 Diabetes Pathogenesis. *Cell Reports*, *31*(1). https://doi.org/10.1016/j.celrep.2020.03.033

Deeney, J. T., Prentki, M., & Corkey, B. E. (2000). Metabolic control of β-cell function. *Seminars in Cell and Developmental Biology*, *11*(4), 267–275. https://doi.org/10.1006/scdb.2000.0175

DiGruccio, M. R., Mawla, A. M., Donaldson, C. J., Noguchi, G. M., Vaughan, J., Cowing-Zitron, C., van der Meulen, T., & Huising, M. O. (2016). Comprehensive alpha, beta and delta cell transcriptomes reveal that ghrelin selectively activates delta cells and promotes somatostatin release from pancreatic islets. *Molecular Metabolism*, *5*(7), 449–458. https://doi.org/10.1016/j.molmet.2016.04.007

Dingreville, F., Panthu, B., Thivolet, C., Ducreux, S., Gouriou, Y., Pesenti, S., Chauvin, M. A., Chikh, K., Errazuriz-Cerda, E., Van Coppenolle, F., Rieusset, J., & Madec, A. M. (2019). Differential effect of glucose on ER-mitochondria Ca2+ exchange participates in insulin secretion and glucotoxicity-mediated dysfunction of β-cells. *Diabetes*, *68*(9), 1778–1794. https://doi.org/10.2337/db18-1112

Fagerberg, L., Hallstrom, B. M., Oksvold, P., Kampf, C., Djureinovic, D., Odeberg, J., Habuka, M., Tahmasebpoor, S., Danielsson, A., Edlund, K., Asplund, A., Sjostedt, E., Lundberg, E., Szigyarto, C. A. K., Skogs, M., Ottosson Takanen, J., Berling, H., Tegel, H., Mulder, J., … Uhlen, M. (2014). Analysis of the human tissue-specific expression by genome-wide integration of transcriptomics and antibody-based proteomics. *Molecular and Cellular Proteomics*, *13*(2), 397–406. https://doi.org/10.1074/mcp.M113.035600

Fex, M., Nicholas, L. M., Vishnu, N., Medina, A., Sharoyko, V. V., Nicholls, D. G., Spégel, P., & Mulder, H. (2018). The pathogenetic role of β-cell mitochondria in type 2 diabetes. In *Journal of Endocrinology* (Vol. 236, Issue 3, pp. R145–R149). BioScientifica Ltd. https://doi.org/10.1530/JOE-17-0367

Fu, Z., Gilbert, E. R., & Liu, D. (2013). Regulation of Insulin Synthesis and Secretion and Pancreatic Beta-Cell Dysfunction in Diabetes. In *Curr Diabetes Rev* (Vol. 9, Issue 1).

Giannuzzi, G., Schmidt, P. J., Porcu, E., Willemin, G., Munson, K. M., Nuttle, X., Earl, R., Chrast, J., Hoekzema, K., Risso, D., Männik, K., De Nittis, P., Baratz, E. D., Herault, Y., Gao, X., Philpott, C. C., Bernier, R. A., Kutalik, Z., Fleming, M. D., … Reymond, A. (2019). The Human-Specific BOLA2 Duplication Modifies Iron Homeostasis and Anemia Predisposition in Chromosome 16p11.2 Autism Individuals. *American Journal of Human Genetics*, *105*(5), 947–958. https://doi.org/10.1016/j.ajhg.2019.09.023

González, F., Zhu, Z., Shi, Z. D., Lelli, K., Verma, N., Li, Q. V., & Huangfu, D. (2014). An iCRISPR platform for rapid, multiplexable, and inducible genome editing in human pluripotent stem cells. *Cell Stem Cell*, *15*(2), 215–226. https://doi.org/10.1016/j.stem.2014.05.018

Guo, S., Dai, C., Guo, M., Taylor, B., Harmon, J. S., Sander, M., Robertson, R. P., Powers, A. C., & Stein, R. (2013). Inactivation of specific β cell transcription factors in type 2 diabetes. *Journal of Clinical Investigation*, *123*(8), 3305–3316. https://doi.org/10.1172/JCI65390

Haack, T. B., Rolinski, B., Haberberger, B., Zimmermann, F., Schum, J., Strecker, V., Graf, E., Athing, U., Hoppen, T., Wittig, I., Sperl, W., Freisinger, P., Mayr, J. A., Strom, T. M., Meitinger, T., & Prokisch, H. (2013). Homozygous missense mutation in BOLA3 causes multiple mitochondrial dysfunctions syndrome in two siblings. *Journal of Inherited Metabolic Disease*, *36*(1), 55–62. https://doi.org/10.1007/s10545-012-9489-7

Hirschberg, P. R., Sarkar, P., Teegala, S. B., & Routh, V. H. (2020). Ventromedial hypothalamus glucose-inhibited neurones: A role in glucose and energy homeostasis? In *Journal of Neuroendocrinology* (Vol. 32, Issue 1). Blackwell

Publishing Ltd. https://doi.org/10.1111/jne.12773

Hou, J. C., Min, L., & Pessin, J. E. (2009). Chapter 16 Insulin Granule Biogenesis, Trafficking and Exocytosis. In *Vitamins and Hormones* (Vol. 80, Issue C, pp. 473–506). https://doi.org/10.1016/S0083-6729(08)00616-X

Imai-Okazaki A, Kishita Y, Kohda M, Mizuno Y, Fushimi T, Matsunaga A, Yatsuka Y, Hirata T, Harashima H, Takeda A, Nakaya A, Sakata Y, Kogaki S, Ohtake A, Murayama K, Okazaki Y. Cardiomyopathy in children with mitochondrial disease: Prognosis and genetic background. Int J Cardiol. 2019 Mar 15;279:115-121. doi: 10.1016/j.ijcard.2019.01.017. Epub 2019 Jan 5. PMID: 30642647.

Jermendy, A., Toschi, E., Aye, T., Koh, A., Aguayo-Mazzucato, C., Sharma, A., Weir, G. C., Sgroi, D., & Bonner-Weir, S. (2011). Rat neonatal beta cells lack the specialised metabolic phenotype of mature beta cells. *Diabetologia*, *54*(3), 594–604. https://doi.org/10.1007/s00125-010-2036-x

Kahn, S. E. (2003). The relative contributions of insulin resistance and beta-cell dysfunction to the pathophysiology of Type 2 diabetes. In *Diabetologia* (Vol. 46, Issue 1, pp. 3–19). Springer Verlag. https://doi.org/10.1007/s00125-002-1009-0

Kahn, Steven E., Hull, R. L., & Utzschneider, K. M. (2006). Mechanisms linking obesity to insulin resistance and type 2 diabetes. In *Nature* (Vol. 444, Issue 7121, pp. 840–846). Nature Publishing Group. https://doi.org/10.1038/nature05482

Kim, A., Miller, K., Jo, J., Kilimnik, G., Wojcik, P., & Hara, M. (2009). Islet architecture: A comparative study. *Islets*, *1*(2), 129–136. https://doi.org/10.4161/isl.1.2.9480

Klemm, D. J., Leitner, J. W., Watson, P., Nesterova, A., Reusch, J. E. B., Goalstone, M. L., & Draznin, B. (2001). Insulin-induced adipocyte differentiation: Activation of CREB rescues adipogenesis from the arrest caused by inhibition of prenylation.

Journal of Biological Chemistry, *276*(30), 28430–28435. https://doi.org/10.1074/jbc.M103382200

Lane, D. J. R., Merlot, A. M., Huang, M. L. H., Bae, D. H., Jansson, P. J., Sahni, S., Kalinowski, D. S., & Richardson, D. R. (2015). Cellular iron uptake, trafficking and metabolism: Key molecules and mechanisms and their roles in disease. In *Biochimica et Biophysica Acta - Molecular Cell Research* (Vol. 1853, Issue 5, pp. 1130–1144). Elsevier. https://doi.org/10.1016/j.bbamcr.2015.01.021

Lebigot, E., Gaignard, P., Dorboz, I., Slama, A., Rio, M., de Lonlay, P., Héron, B., Sabourdy, F., Boespflug-Tanguy, O., Cardoso, A., Habarou, F., Ottolenghi, C., Thérond, P., Bouton, C., Golinelli-Cohen, M. P., & Boutron, A. (2017). Impact of mutations within the [Fe-S] cluster or the lipoic acid biosynthesis pathways on mitochondrial protein expression profiles in fibroblasts from patients. *Molecular Genetics and Metabolism*, *122*(3), 85–94. https://doi.org/10.1016/j.ymgme.2017.08.001

Levi, S., & Rovida, E. (2009). The role of iron in mitochondrial function. In *Biochimica et Biophysica Acta - General Subjects* (Vol. 1790, Issue 7, pp. 629–636). https://doi.org/10.1016/j.bbagen.2008.09.008

Lill, R. (2009). Function and biogenesis of iron-sulphur proteins. In *Nature* (Vol. 460, Issue 7257, pp. 831–838). https://doi.org/10.1038/nature08301

Lill, R., Dutkiewicz, R., Elsässer, H. P., Hausmann, A., Netz, D. J. A., Pierik, A. J., Stehling, O., Urzica, E., & Mühlenhoff, U. (2006). Mechanisms of iron-sulfur protein maturation in mitochondria, cytosol and nucleus of eukaryotes. In *Biochimica et Biophysica Acta - Molecular Cell Research* (Vol. 1763, Issue 7, pp. 652–667). https://doi.org/10.1016/j.bbamcr.2006.05.011

Lu, H., Koshkin, V., Allister, E. M., Gyulkhandanyan, A. V., & Wheeler, M. B. (2010). Molecular and metabolic evidence for mitochondrial defects associated with β-cell dysfunction in a mouse model of type 2 diabetes. *Diabetes*, *59*(2), 448–459. https://doi.org/10.2337/db09-0129

Mayr, J. A., Feichtinger, R. G., Tort, F., Ribes, A., & Sperl, W. (2014). Lipoic acid biosynthesis defects. *Journal of Inherited Metabolic Disease*, *37*(4), 553–563. https://doi.org/10.1007/s10545-014-9705-8

Mulder, H. (2017). Transcribing β-cell mitochondria in health and disease. In *Molecular Metabolism* (Vol. 6, Issue 9, pp. 1040–1051). Elsevier GmbH. https://doi.org/10.1016/j.molmet.2017.05.014

Nair, G. G., Liu, J. S., Russ, H. A., Tran, S., Saxton, M. S., Chen, R., Juang, C., Li, M. lan, Nguyen, V. Q., Giacometti, S., Puri, S., Xing, Y., Wang, Y., Szot, G. L., Oberholzer, J., Bhushan, A., & Hebrok, M. (2019). Recapitulating endocrine cell clustering in culture promotes maturation of human stem-cell-derived β cells. *Nature Cell Biology*, *21*(2), 263–274. https://doi.org/10.1038/s41556-018-0271-4

Osundiji, M. A., Lam, D. D., Shaw, J., Yueh, C. Y., Markkula, S. P., Hurst, P., Colliva, C., Roda, A., Heisler, L. K., & Evans, M. L. (2012). Brain glucose sensors play a significant role in the regulation of pancreatic glucose-stimulated insulin secretion. *Diabetes*, *61*(2), 321–328. https://doi.org/10.2337/db11-1050

Paoletti, R. (n.d.). *ADVANCES IN EXPERIMENTAL MEDICINE AND BIOLOGY*. http://www.springer.com/series/5584

Puri, S., Akiyama, H., & Hebrok, M. (2013). VHL-mediated disruption of Sox9 activity compromises β-cell identity and results in diabetes mellitus. *Genes and Development*, *27*(23), 2563–2575. https://doi.org/10.1101/gad.227785.113

Puri, S., Cano, D. A., & Hebrok, M. (2009). A role for von hippel-lindau protein in pancreatic β-cell function. *Diabetes*, *58*(2), 433–441. https://doi.org/10.2337/db08-0749

Puri, S., Folias, A. E., & Hebrok, M. (2015). Plasticity and dedifferentiation within the pancreas: Development, homeostasis, and disease. In *Cell Stem Cell* (Vol. 16, Issue 1, pp. 18–31). Cell Press. https://doi.org/10.1016/j.stem.2014.11.001

Puri, S., García-Núñez, A., Hebrok, M., & Cano, D. A. (2013). Elimination of Von Hippel-Lindau Function Perturbs Pancreas Endocrine Homeostasis in Mice. *PLoS ONE*, *8*(8). https://doi.org/10.1371/journal.pone.0072213

Puri, S., Roy, N., Russ, H. A., Leonhardt, L., French, E. K., Roy, R., Bengtsson, H., Scott, D. K., Stewart, A. F., & Hebrok, M. (2018). Replication confers β cell immaturity. *Nature Communications*, *9*(1). https://doi.org/10.1038/s41467-018-02939-0

Randle PJ. Mitochondrial 2-oxoacid dehydrogenase complexes of animal tissues. Philos Trans R Soc Lond B Biol Sci. 1983 Jul 5;302(1108):47-57. doi: 10.1098/rstb.1983.0037. PMID: 6137008.

Rouault, T. A. (2015). Mammalian iron-sulphur proteins: Novel insights into biogenesis and function. In *Nature Reviews Molecular Cell Biology* (Vol. 16, Issue 1, pp. 45–55). Nature Publishing Group. https://doi.org/10.1038/nrm3909

Rouault, T. A., & Tong, W. H. (2008). Iron-sulfur cluster biogenesis and human disease. In *Trends in Genetics* (Vol. 24, Issue 8, pp. 398–407). https://doi.org/10.1016/j.tig.2008.05.008

Routh, V. H., Hao, L., Santiago, A. M., Sheng, Z., & Zhou, C. (2014). Hypothalamic glucose sensing: Making ends meet. In *Frontiers in Systems Neuroscience* (Vol. 8,

Issue DEC). Frontiers Media S.A. https://doi.org/10.3389/fnsys.2014.00236

Sato, Y., Inoue, M., Yoshizawa, T., & Yamagata, K. (2014). Moderate hypoxia induces β-cell dysfunction with HIF-1-independent gene expression changes. *PLoS ONE*, *9*(12). https://doi.org/10.1371/journal.pone.0114868

Seino, S., Shibasaki, T., & Minami, K. (2011). Dynamics of insulin secretion and the clinical implications for obesity and diabetes. In *Journal of Clinical Investigation* (Vol. 121, Issue 6, pp. 2118–2125). https://doi.org/10.1172/JCI45680

Shyr, Z. A., Wang, Z., York, N. W., Nichols, C. G., & Remedi, M. S. (2019). The role of membrane excitability in pancreatic β-cell glucotoxicity. *Scientific Reports*, *9*(1). https://doi.org/10.1038/s41598-019-43452-8

Simcox, J. A., & McClain, D. A. (2013). Iron and diabetes risk. In *Cell Metabolism* (Vol. 17, Issue 3, pp. 329–341). https://doi.org/10.1016/j.cmet.2013.02.007

Steiner, D. J., Kim, A., Miller, K., & Hara, M. (n.d.). *Pancreatic islet plasticity: Interspecies comparison of islet architecture and composition*.

Supale, S., Li, N., Brun, T., & Maechler, P. (2012). Mitochondrial dysfunction in pancreatic β cells. In *Trends in Endocrinology and Metabolism* (Vol. 23, Issue 9, pp. 477–487). https://doi.org/10.1016/j.tem.2012.06.002

Swaminathan, S., Fonseca, V. A., Alam, M. G., & Shah, S. V. (2007). The role of iron in diabetes and its complications. In *Diabetes Care* (Vol. 30, Issue 7, pp. 1926–1933). https://doi.org/10.2337/dc06-2625

Tajima, K., Ikeda, K., Chang, H. Y., Chang, C. H., Yoneshiro, T., Oguri, Y., Jun, H., Wu, J., Ishihama, Y., & Kajimura, S. (2019). Mitochondrial lipoylation integrates age-associated decline in brown fat thermogenesis. *Nature Metabolism*, *1*(9), 886–898. https://doi.org/10.1038/s42255-019-0106-z

Talchai, C., Xuan, S., Lin, H. V., Sussel, L., & Accili, D. (2012). Pancreatic β cell dedifferentiation as a mechanism of diabetic β cell failure. *Cell*, *150*(6), 1223–1234. https://doi.org/10.1016/j.cell.2012.07.029

Tarasov, A., Dusonchet, J., & Ashcroft, F. (2004). Metabolic Regulation of the Pancreatic-Cell ATP-Sensitive K Channel A Pas de Deux. In *DIABETES* (Vol. 53).

Thivolet, C., Vial, G., Cassel, R., Rieusset, J., & Madec, A. M. (2017). Reduction of endoplasmic reticulum-mitochondria interactions in beta cells from patients with type 2 diabetes. *PLoS ONE*, *12*(7). https://doi.org/10.1371/journal.pone.0182027

Uhlén, M., Fagerberg, L., Hallström, B. M., Lindskog, C., Oksvold, P., Mardinoglu, A., Sivertsson, Å., Kampf, C., Sjöstedt, E., Asplund, A., Olsson, I. M., Edlund, K., Lundberg, E., Navani, S., Szigyarto, C. A. K., Odeberg, J., Djureinovic, D., Takanen, J. O., Hober, S., … Pontén, F. (2015). Tissue-based map of the human proteome. *Science*, *347*(6220). https://doi.org/10.1126/science.1260419

Wang, Z., York, N. W., Nichols, C. G., & Remedi, M. S. (2014). Pancreatic β cell dedifferentiation in diabetes and redifferentiation following insulin therapy. *Cell Metabolism*, *19*(5), 872–882. https://doi.org/10.1016/j.cmet.2014.03.010

Wicksteed, B., Brissova, M., Yan, W., Opland, D. M., Plank, J. L., Reinert, R. B., Dickson, L. M., Tamarina, N. A., Philipson, L. H., Shostak, A., Bernal-Mizrachi, E., Elghazi, L., Roe, M. W., Labosky, P. A., Myers, M. G., Gannon, M., Powers, A. C., & Dempsey, P. J. (2010). Conditional gene targeting in mouse pancreatic β-cells: Analysis of ectopic cre transgene expression in the brain. *Diabetes*, *59*(12), 3090–3098. https://doi.org/10.2337/db10-0624

Willems, P., Wanschers, B. F. J., Esseling, J., Szklarczyk, R., Kudla, U., Duarte, I., Forkink, M., Nooteboom, M., Swarts, H., Gloerich, J., Nijtmans, L., Koopman, W., &

Huynen, M. A. (2013). BOLA1 is an aerobic protein that prevents mitochondrial morphology changes induced by glutathione depletion. *Antioxidants and Redox Signaling*, *18*(2), 129–138. https://doi.org/10.1089/ars.2011.4253

Yeaman, S. J. (1989). The 2-oxo acid dehydrogenase complexes: recent advances. In *Biochem. J* (Vol. 257).

Zhang, H. H., Huang, J., Düvel, K., Boback, B., Wu, S., Squillance, R. M., Wu, C. L., & Manning, B. D. (2009). Insulin stimulates adipogenesis through the Akt-TSC2-mTORC1 pathway. *PLoS ONE*, *4*(7). https://doi.org/10.1371/journal.pone.0006189

Zhou, Y. B., Cao, J. B., Wan, B. B., Wang, X. R., Ding, G. H., Zhu, H., Yang, H. M., Wang, K. S., Zhang, X., & Han, Z. G. (2008). hBolA, novel non-classical secreted proteins, belonging to different BolA family with functional divergence. *Molecular and Cellular Biochemistry*, *317*(1–2), 61–68. https://doi.org/10.1007/s11010-008-9809-2

Publishing Agreement

It is the policy of the University to encourage open access and broad distribution of all theses, dissertations, and manuscripts. The Graduate Division will facilitate the distribution of UCSF theses, dissertations, and manuscripts to the UCSF Library for open access and distribution. UCSF will make such theses, dissertations, and manuscripts accessible to the public and will take reasonable steps to preserve these works in perpetuity.

I hereby grant the non-exclusive, perpetual right to The Regents of the University of California to reproduce, publicly display, distribute, preserve, and publish copies of my thesis, dissertation, or manuscript in any form or media, now existing or later derived, including access online for teaching, research, and public service purposes.

DocuSigned by:
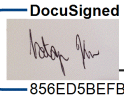
856ED5BEFB2E484...

Author Signature

9/2/2021
Date